# SUPPLEMENTARY INFORMATION

## Interactions of Hydrophilic Birch Wood (*Betula pendula* ROTH) Extractives with Adhesives for Load-bearing Timber Structures

**Journal:** International Journal of Adhesion and Adhesives

**Authors:**

Max ENGELHARDT[1,*]
orcid.org/0000-0002-9781-7476 (engelhardt@hfm.tum.de)

Thomas BÖGER[1]
orcid.org/0000-0001-8747-8506 (boeger@hfm.tum.de)

Michael GIGL[2]
orcid.org/0000-0002-5617-9236 (michael.gigl@tum.de)

Chen MENG[2]
orcid.org/0000-0002-5968-6719 (chen.meng@tum.de)

Viktor SOPRUNYUK[3]
orcid.org/0000-0001-7073-6900 (viktor.soprunyuk@univie.ac.at)

Wilfried SCHRANZ[3]
orcid.org/0000-0002-9842-3532 (wilfried.schranz@univie.ac.at)

Klaus RICHTER[1]
orcid.org/0000-0002-6583-0254 (richter@hfm.tum.de)

Antoni SÁNCHEZ-FERRER[1,*]
orcid.org/0000-0002-1041-0324 (sanchez@hfm.tum.de)

[1] Chair of Wood Science, TUM School of Life Sciences, Technical University of Munich

[2] Bavarian Center for Biomolecular Mass Spectrometry, TUM School of Life Sciences, Technical University Munich

[3] Faculty of Physics, University of Vienna

## Figures



## Tables

## Experimental Section – Tensile Shear Strength Experiments

Table SI–1 lists the relevant bonding processing parameters (conducted at 20 °C/65%-RH).

Table SI–1: Bonding parameters for the applied adhesive systems

| **adhesive type** | **PUR** | **MUF** |
|---|---|---|
| quantity [g/m²] | 175 – 180 | 375 – 385 |
| open waiting time [min] | 1 – 2 | 2 – 4 |
| closed waiting time [min] | 20 ± 4 | 40 ± 5 |
| pressure [MPa] | 0.8 | 1.2 |
| pressing time [h] | 1.5 | 10 |
| application | toothed spatula, single-sided | toothed spatula, both-sided |

Table SI–2 lists the treatments applied to the specimens after bonding.

Table SI–2: Applied treatment procedures of tensile shear specimens as defined in EN 302–1

| **designation** | **treatment description** | **measurement conditions** |
|---|---|---|
| **A1** | equilibrate at standard climate (20 °C/65%-RH) | standard climate (20 °C/65%-RH) |
| **A2** | A1 + 4 days soaking in cold water at 20 °C | wet state |
| **A4** | A1 + 6 h soaking in boiling water, 2 h soaking in cold water (20 °C) | wet state |
| **A5** | A1 + 6 h soaking in boiling water, 2 h soaking in cold water (20 °C) | recondition in standard climate |

The tensile shear specimen geometry and loading schematic and the cutting pattern of specimens prepared from the glued boards are shown in Figure SI–1.

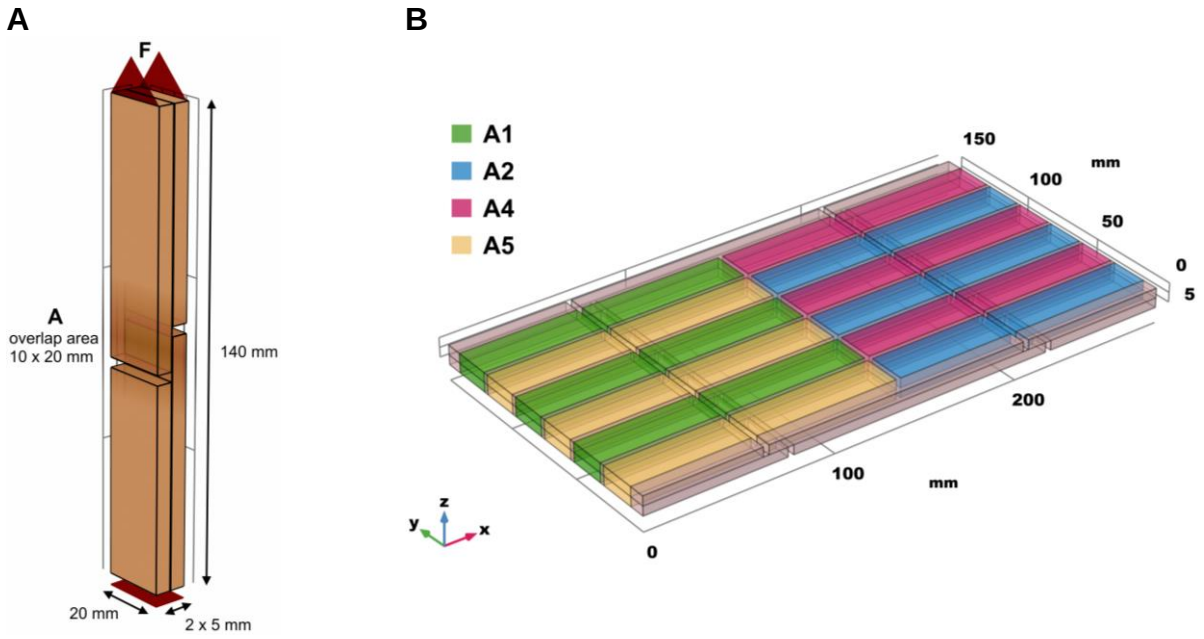


Figure SI–1: A) Tensile shear strength specimen acc. to EN 302–1. B) Cutting pattern of tensile shear specimens from glued boards. Color indication of treatment type (designation code acc. to EN 302–1).

## Experimental Section – Rheological Experiments of Isothermal Curing

The determination of gelation *via* multi-frequency time-sweep in a small-angle-oscillatory-shear (SAOS) experiment is visualized in Figure SI–2 below. Figure SI–2A shows the progression of the loss factor tan δ for different oscillation frequencies $f$. In Figure SI–2B, for selected times / frequency sweep cycles, the loss factors tan δ (detrended) are plotted as a function of $f$. While regression analysis shows positive slopes prior to gelation and negative slopes after gelation ($\tan\delta \propto f^n$), the gel point is identified as the time when the slope is zero (n = 0) by calculating the variance of tan δ and finding the local minimum (Figure SI–2C).

The gel point can be identified in (A) by the temporary convergence of the loss factors, in (B) by constant loss factor values and resulting horizontal regression line of zero slope value and in (C) by the local minimum of loss factor variance s², each shown using pink color. The crossover, when tan δ = 1, can be seen occurring at considerably later times and depending on the frequency considered (dashed lines in (A)).

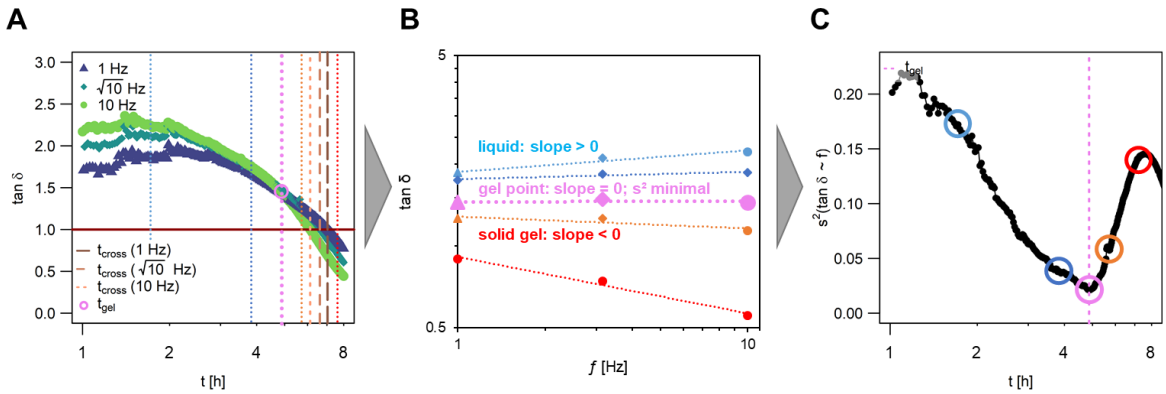


Figure SI–2: Schematic of gel time evaluation using multi-frequency SAOS experiments. A: progression of tan δ for the frequencies 1 Hz, $\sqrt{10}$ Hz and 10 Hz. Dark and light blue, pink, orange and red dotted lines in (A) correspond to the respective colored frequency cycle data in (B) and loss factor variance s² in (C).

## Results and Discussion – Chemical Characteristics of Extractives

The concentrations of saccharides as measured by LC sugar analyzer are listed in Table SI–3. The chemical compounds in the birch wood extractive (cold-water extraction), classified as compound types per GC-MS analysis and estimated concentrations via the internal standard of the birch extractive sample used in this study, are listed in Table SI–4. The compounds, as classified into compound types per UHPLC-ESI-TOF-MS analysis with abundance (peak area), are listed in Table SI–5, whereby high-precision MS data is given as median m/z of the parent ion with 4 digits to 0.0001 Da.

Table SI–3: Free and hydrolyzed saccharide concentrations in birch wood cold-water extractive as identified per LC sugar analyzer using different methods of hydrolysis

| **saccharide** | **concentration [mg/g]** | |
|---|---|---|
| | hydrolysis method I | hydrolysis method II |
| Oligosaccharides[#] | 3.59 | 2.59 |
| cellobiose | 1.2 | < 1 |
| Rhamnose | 2.62 | 2.74 |
| peak at 16 min° | < 1 | < 1 |
| Mannose | 3.38 | 3.83 |
| peak at 24 min+ | 2.59 | --- |
| Arabinose | 4.98 | 4.07 |
| Galactose | 4.25 | 4.21 |
| Xylose | 15.08 | 11.71 |
| Glucose | 39.75 | 45.04 |
| total | 77.44 | 74.19 |

#Oligo calculated as Cellobiose
°calculated as Rhamnose
+calculated as Arabinose

In the study, the higher results of the hydrolysis method per saccharide are considered, giving a total of 81.1 mg/g.

Table SI–4: Gas-chromatography coupled with mass spectrometry (GC-MS) on silylated water extract sample of silver birch (*Betula pendula* Roth) – Most abundant compounds. Qual: NIST MS Search reported quality. Concentrations and molar mass calculated via peak area (derivatized) using an internal standard (heneicosanoic acid) were corrected for silylation weight gain.

| $t_R$ [min] | compound type | silylated concentration [µg/mL] | concentration [µg/mL] | concentration [mg/g] | concentration in wood [µg/g] | molar mass [Da] |
|---|---|---|---|---|---|---|
| 12.62 | Saccharide (mono) | 300.2 | 99.9 | 25.2 | 353.3 | 180.2 |
| 10.29 | Saccharide (mono) | 114.4 | 39.2 | 9.9 | 138.4 | 150.1 |
| 10.90 | Fatty Acid and Conjugates (Carboxylic acid) | 48.3 | 27.3 | 6.9 | 96.6 | 188.2 |
| 10.84 | Saccharide (mono) | 80.1 | 26.7 | 6.7 | 94.1 | 180.2 |
| 10.80 | Saccharide (mono) | 53.3 | 17.8 | 4.5 | 62.8 | 180.2 |
| 11.68 | Saccharide (mono) | 31.8 | 10.6 | 2.7 | 37.4 | 180.2 |
| 10.71 | Saccharide (mono) | 20.9 | 7.2 | 1.8 | 25.3 | 150.1 |
| 4.73 | Polyol | 30.7 | 9.2 | 2.3 | 32.3 | 92.1 |
| 5.87 | Fatty Acid and Conjugates (Carboxylic acid) | 11.8 | 7.9 | 2.0 | 27.9 | 146.2 |
| 8.70 | Fatty Acid and Conjugates (Carboxylic acid) | 15.6 | 6.9 | 1.7 | 24.5 | 116.1 |
| 10.95 | Fatty Acid and Conjugates (Dicarboxylic acid) | 13.2 | 6.1 | 1.5 | 21.5 | 187.2 |
| 9.86 | Fatty Acid and Conjugates (Dicarboxylic acid) | 9.4 | 5.2 | 1.3 | 18.2 | 174.2 |
| 19.69 | Fatty Acid and Conjugates (Carboxylic acid) | 9.1 | 3.4 | 0.9 | 11.9 | 170.1 |
| 8.93 | Fatty Acid and Conjugates (Carboxylic acid) | 12.1 | 4.4 | 1.1 | 15.5 | 74.1 |
| 8.57 | Saccharide (mono) | 17.0 | 5.4 | 1.4 | 19.2 | 136.1 |
| 11.76 | Saccharide (mono) | 14.7 | 5.1 | 1.3 | 18.2 | 180.2 |
| 12.41 | Polyol | 5.6 | 3.1 | 0.8 | 11.1 | 180.2 |
| 13.50 | Polyol | 8.6 | 2.5 | 0.6 | 9.0 | 180.2 |
| 18.60 | Fatty Acid and Conjugates (Carboxylic acid) | 5.2 | 2.0 | 0.5 | 7.0 | 89.1 |
| 5.17 | Fatty Acid and Conjugates (Carboxylic acid) | 6.1 | 2.4 | 0.6 | 8.3 | 100.1 |
| 8.82 | Fatty Acid and Conjugates (Dicarboxylic acid) | 3.2 | 1.7 | 0.4 | 6.0 | 160.2 |
| 11.59 | Saccharide (mono) | 3.3 | 1.1 | 0.3 | 4.0 | 150.1 |
| 17.34 | Saccharide (mono) | 3.0 | 1.0 | 0.2 | 3.4 | 150.1 |
| 7.20 | Fatty Acid and Conjugates (Dicarboxylic acid) | 2.2 | 1.0 | 0.3 | 3.6 | 190.1 |
| 12.51 | Saccharide (mono) | 1.9 | 0.7 | 0.2 | 2.3 | 150.1 |

Table SI–5: List of compound features detected via UHPLC-ESI-TOF-MS analysis of birch wood amphiphilic and hydrophilic extractives with retention time, mass-to-charge ratio, compound type annotation and TIC abundance values.

| $t_R$ [s] | m/z [Da] | compound type | abundance (peak area) |
|---|---|---|---|
| 41.01 | 1080.7848 | Saccharide | 74620 |
| 41.01 | 944.8092 | Saccharide | 97804 |
| 41.08 | 808.8334 | Saccharide | 132950 |
| 41.08 | 876.8216 | Saccharide | 116307 |
| 41.16 | 740.8462 | Saccharide | 135039 |
| 41.16 | 834.8401 | Saccharide | 58090 |
| 41.16 | 1004.8091 | Saccharide | 47667 |
| 41.24 | 902.8279 | Saccharide | 55629 |
| 41.24 | 800.8458 | Saccharide | 48529 |
| 41.24 | 766.8540 | Saccharide | 39251 |
| 41.26 | 868.8343 | Saccharide | 57409 |
| 41.27 | 672.8582 | Saccharide | 128712 |
| 41.29 | 604.8706 | Saccharide | 135104 |
| 41.29 | 536.8827 | Phenyl glycoside | 109451 |
| 47.40 | 211.0817 | Saccharide | 7072 |
| 47.76 | 179.0559 | Saccharide | 44881 |
| 48.98 | 195.0513 | Saccharide | 2663623 |
| 49.99 | 711.2203 | Saccharide | 13227 |
| 50.10 | 665.2148 | Saccharide | 10351 |
| 50.38 | 341.1088 | Saccharide | 15580 |
| 50.47 | 503.1607 | Saccharide | 22223 |
| 52.36 | 379.0831 | Saccharide | 1996 |
| 52.37 | 377.0857 | Saccharide | 5902 |
| 54.78 | 96.9606 | Inorganic Acid | 21601 |
| 82.17 | 96.9607 | Inorganic Acid | 50403 |
| 197.22 | 451.1445 | Phenyl glycoside | 106263 |
| 197.48 | 737.2363 | Phenyl glycoside | 133362 |
| 203.64 | 161.0815 | Fatty Acid and Conjugates | 89200 |
| 208.71 | 169.0141 | Phenol | 1471 |
| 209.70 | 391.1238 | Phenyl glycoside | 40403 |
| 210.51 | 460.1504 | Phenyl glycoside | 38749 |
| 210.82 | 203.0922 | Fatty Acid and Conjugates | 31509 |
| 210.86 | 459.1490 | Phenyl glycoside | 171298 |
| 211.90 | 175.0957 | Fatty Acid and Conjugates | 235182 |
| 212.09 | 176.1004 | Fatty Acid and Conjugates | 19615 |
| 212.34 | 451.1456 | Phenyl glycoside | 2092 |
| 212.69 | 189.0771 | Fatty Acid and Conjugates | 88321 |
| 213.54 | 359.0985 | Phenyl glycoside | 200188 |
| 215.72 | 215.0919 | Fatty Acid and Conjugates | 18326 |
| 215.94 | 195.0663 | Phenol | 1445 |
| 216.65 | 173.0816 | Fatty Acid and Conjugates | 29607 |
| 217.01 | 445.1757 | Phenyl glycoside | 203704 |
| 218.01 | 447.1168 | Phenyl glycoside | 19064 |
| 218.43 | 405.1395 | Phenyl glycoside | 74974 |
| 218.43 | 217.1077 | Fatty Acid and Conjugates | 289911 |
| 218.86 | 199.0969 | Fatty Acid and Conjugates | 45198 |
| 218.94 | 201.0765 | Fatty Acid and Conjugates | 32258 |
| 220.78 | 461.1285 | Phenyl glycoside | 15071 |

Table SI–5: List of compound features detected via UHPLC-ESI-TOF-MS analysis of birch wood amphiphilic and hydrophilic extractives with retention time, mass-to-charge ratio, compound type annotation and TIC abundance values. (CONTINUED)

| $t_R$ [s]] | m/z [Da] | compound type | abundance (peak area) |
|---|---|---|---|
| 221.01 | 444.1935 | Phenyl glycoside | 259914 |
| 221.05 | 443.1914 | Phenyl glycoside | 1197706 |
| 221.62 | 551.1607 | Phenyl glycoside | 11064 |
| 224.94 | 521.1006 | Phenyl glycoside | 7433 |
| 225.36 | 241.0718 | Phenol | 31482 |
| 225.36 | 489.1652 | Phenyl glycoside | 35886 |
| 226.31 | 203.0929 | Fatty Acid and Conjugates | 312996 |
| 226.69 | 527.1751 | Phenyl glycoside | 123993 |
| 226.95 | 557.1849 | Phenyl glycoside | 47988 |
| 229.31 | 161.0813 | Fatty Acid and Conjugates | 22639 |
| 229.99 | 541.1585 | Phenyl glycoside | 31160 |
| 230.76 | 523.1666 | Phenyl glycoside | 842357 |
| 230.76 | 524.1700 | Phenyl glycoside | 189947 |
| 230.83 | 525.1722 | Phenyl glycoside | 68070 |
| 230.83 | 577.0860 | Phenyl glycoside | 13784 |
| 230.98 | 513.1374 | Phenyl glycoside | 40377 |
| 230.99 | 575.1285 | Phenyl glycoside | 40968 |
| 231.01 | 540.1559 | Phenyl glycoside | 23962 |
| 231.01 | 515.1350 | Phenyl glycoside | 12266 |
| 231.01 | 576.0819 | Phenyl glycoside | 11727 |
| 231.05 | 591.1529 | Phenyl glycoside | 22552 |
| 231.26 | 478.1636 | Phenyl glycoside | 25070 |
| 231.33 | 477.1611 | Phenyl glycoside | 112230 |
| 231.37 | 693.2607 | Phenyl glycoside | 39947 |
| 231.42 | 479.1652 | Phenyl glycoside | 13471 |
| 231.86 | 215.0925 | Fatty Acid and Conjugates | 102624 |
| 233.45 | 505.1906 | Phenyl glycoside | 154065 |
| 233.98 | 427.1583 | Phenyl glycoside | 183186 |
| 234.44 | 507.1862 | Phenyl glycoside | 546173 |
| 234.45 | 391.1245 | Phenyl glycoside | 392164 |
| 234.86 | 503.1754 | Phenyl glycoside | 44530 |
| 235.68 | 509.1892 | Phenyl glycoside | 39956 |
| 235.68 | 625.1236 | Phenyl glycoside | 15021 |
| 236.08 | 585.1818 | Phenyl glycoside | 331447 |
| 236.14 | 586.1844 | Phenyl glycoside | 98557 |
| 237.59 | 583.2013 | Phenyl glycoside | 68822 |
| 237.80 | 201.0785 | Fatty Acid and Conjugates | 63634 |
| 238.62 | 401.1443 | Phenyl glycoside | 39028 |
| 238.86 | 447.1511 | Phenyl glycoside | 54938 |
| 240.08 | 319.1193 | Polyphenol | 51753 |
| 240.39 | 555.1711 | Phenyl glycoside | 330303 |
| 240.49 | 271.0963 | Polyphenol | 42911 |
| 240.84 | 287.1503 | Fatty Acid and Conjugates | 9787 |
| 241.21 | 301.1113 | Polyphenol | 25079 |
| 241.43 | 245.1354 | Fatty Acid and Conjugates | 33948 |
| 241.82 | 627.2230 | Phenyl glycoside | 12252 |
| 242.23 | 443.1918 | Phenyl glycoside | 1032781 |
| 242.23 | 444.1953 | Phenyl glycoside | 224539 |
| 242.64 | 541.1584 | Phenyl glycoside | 26346 |

Table SI–5: List of compound features detected via UHPLC-ESI-TOF-MS analysis of birch wood amphiphilic and hydrophilic extractives with retention time, mass-to-charge ratio, compound type annotation and TIC abundance values. (CONTINUED)

| **$t_R$ [s]]** | **m/z [Da]** | **compound type** | **abundance (peak area)** |
|---|---|---|---|
| 242.68 | 432.1948 | Glycolipid | 184873 |
| 242.68 | 431.1916 | Glycolipid | 884015 |
| 242.69 | 159.0664 | Fatty Acid and Conjugates | 86052 |
| 242.84 | 161.0816 | Fatty Acid and Conjugates | 57655 |
| 243.28 | 567.1768 | Phenyl glycoside | 45929 |
| 243.98 | 423.1795 | Glycolipid | 160300 |
| 244.15 | 539.1417 | Phenyl glycoside | 29736 |
| 244.96 | 517.2580 | Glycolipid | 72309 |
| 246.12 | 195.0660 | Phenol | 21554 |
| 246.14 | 491.0856 | Phenyl glycoside | 3063 |
| 247.27 | 557.1568 | Phenyl glycoside | 80844 |
| 247.39 | 573.1758 | Phenyl glycoside | 63371 |
| 247.39 | 527.1716 | Phenyl glycoside | 57573 |
| 247.43 | 459.1871 | Phenyl glycoside | 4800610 |
| 247.52 | 460.1898 | Phenyl glycoside | 1020254 |
| 247.67 | 495.1623 | Phenyl glycoside | 87130 |
| 247.77 | 461.1834 | Phenyl glycoside | 217071 |
| 248.24 | 787.2676 | Phenyl glycoside | 59673 |
| 248.25 | 788.2701 | Phenyl glycoside | 22178 |
| 248.46 | 505.1912 | Phenyl glycoside | 129033 |
| 249.81 | 579.2054 | Phenyl glycoside | 89178 |
| 250.08 | 465.1033 | Phenyl glycoside | 2677 |
| 250.19 | 569.1855 | Phenyl glycoside | 234351 |
| 252.65 | 580.2104 | Phenyl glycoside | 39570 |
| 252.80 | 489.1366 | Phenyl glycoside | 11491 |
| 252.96 | 203.0927 | Fatty Acid and Conjugates | 75790 |
| 253.07 | 391.1372 | Phenyl glycoside | 6520 |
| 253.29 | 553.1795 | Phenyl glycoside | 101700 |
| 254.30 | 515.1897 | Polyphenol | 71312 |
| 254.75 | 585.2184 | Phenyl glycoside | 182709 |
| 254.75 | 586.2212 | Phenyl glycoside | 52905 |
| 255.27 | 549.1918 | Phenyl glycoside | 111582 |
| 256.06 | 581.2240 | Phenyl glycoside | 2219749 |
| 256.06 | 627.2291 | Phenyl glycoside | 914613 |
| 256.06 | 582.2264 | Phenyl glycoside | 631063 |
| 256.13 | 628.2322 | Phenyl glycoside | 283610 |
| 256.25 | 521.2018 | Phenyl glycoside | 555452 |
| 256.43 | 419.1154 | Phenyl glycoside | 48415 |
| 256.47 | 583.2223 | Phenyl glycoside | 196023 |
| 256.55 | 261.1343 | Glycerolipid | 65138 |
| 256.67 | 447.1022 | Phenyl glycoside | 8795 |
| 258.46 | 541.1495 | Phenyl glycoside | 69859 |
| 259.01 | 539.1433 | Phenyl glycoside | 486430 |
| 259.05 | 540.1451 | Phenyl glycoside | 120723 |
| 259.06 | 517.1921 | Phenyl glycoside | 18415 |
| 259.13 | 525.1607 | Phenyl glycoside | 190894 |
| 261.21 | 491.1913 | Phenyl glycoside | 424277 |
| 262.09 | 509.1307 | Phenyl glycoside | 391926 |

Table SI–5: List of compound features detected via UHPLC-ESI-TOF-MS analysis of birch wood amphiphilic and hydrophilic extractives with retention time, mass-to-charge ratio, compound type annotation and TIC abundance values. (CONTINUED)

| **$t_R$ [s]** | **m/z [Da]** | **compound type** | **abundance (peak area)** |
|---|---|---|---|
| 262.11 | 567.2067 | Phenyl glycoside | 141812 |
| 262.38 | 247.1189 | Glycerolipid | 337389 |
| 263.98 | 185.0820 | Fatty Acid and Conjugates | 49254 |
| 264.87 | 713.2662 | Phenyl glycoside | 36484 |
| 266.82 | 577.1926 | Phenyl glycoside | 45353 |
| 267.18 | 595.2032 | Phenyl glycoside | 711661 |
| 267.31 | 596.2058 | Phenyl glycoside | 212146 |
| 267.43 | 551.2137 | Phenyl glycoside | 770497 |
| 267.43 | 552.2160 | Phenyl glycoside | 218667 |
| 267.49 | 597.2171 | Phenyl glycoside | 463304 |
| 267.56 | 598.2204 | Phenyl glycoside | 132193 |
| 268.50 | 261.1344 | Glycerolipid | 115304 |
| 268.74 | 449.2010 | Phenyl glycoside | 322027 |
| 269.09 | 475.1972 | Phenyl glycoside | 266713 |
| 269.26 | 451.1264 | Phenyl glycoside | 109013 |
| 269.87 | 489.1746 | Phenyl glycoside | 692178 |
| 271.37 | 481.1344 | Phenyl glycoside | 283517 |
| 271.38 | 459.1474 | Phenyl glycoside | 21988 |
| 271.65 | 173.0820 | Fatty Acid and Conjugates | 470543 |
| 271.82 | 195.0639 | Fatty Acid and Conjugates | 11408 |
| 272.04 | 523.1387 | Phenyl glycoside | 2552 |
| 272.06 | 513.1757 | Phenyl glycoside | 6857 |
| 274.10 | 423.1299 | Phenyl glycoside | 51011 |
| 275.24 | 205.1081 | Fatty Acid and Conjugates | 361501 |
| 275.67 | 159.1020 | Fatty Acid and Conjugates | 203168 |
| 275.77 | 569.2213 | Phenyl glycoside | 84031 |
| 275.84 | 521.2013 | Phenyl glycoside | 99493 |
| 276.05 | 431.1365 | Phenyl glycoside | 16760 |
| 276.09 | 553.1899 | Phenyl glycoside | 160960 |
| 276.64 | 611.1965 | Phenyl glycoside | 27509 |
| 276.95 | 495.1496 | Phenyl glycoside | 268226 |
| 278.44 | 573.2032 | Phenyl glycoside | 22126 |
| 279.15 | 549.2529 | Phenyl glycoside | 81965 |
| 279.29 | 245.1392 | Fatty Acid and Conjugates | 8479 |
| 279.73 | 551.2133 | Phenyl glycoside | 53286 |
| 279.73 | 552.2162 | Phenyl glycoside | 13937 |
| 280.18 | 217.1083 | Fatty Acid and Conjugates | 194732 |
| 280.71 | 593.2051 | Phenyl glycoside | 18190 |
| 281.36 | 461.0739 | Phenyl glycoside | 1614 |
| 282.18 | 579.2077 | Phenyl glycoside | 809362 |
| 282.32 | 580.2106 | Phenyl glycoside | 241517 |
| 282.38 | 427.1584 | Phenyl glycoside | 4485 |
| 283.03 | 449.1449 | Phenyl glycoside | 2721 |
| 283.21 | 505.1335 | Phenyl glycoside | 2807 |
| 283.31 | 625.2132 | Phenyl glycoside | 166867 |
| 283.63 | 515.1765 | Phenyl glycoside | 41472 |
| 283.74 | 175.0971 | Fatty Acid and Conjugates | 1134999 |
| 283.74 | 176.1006 | Fatty Acid and Conjugates | 93180 |
| 284.26 | 496.1174 | Phenyl glycoside | 67627 |

Table SI–5: List of compound features detected via UHPLC-ESI-TOF-MS analysis of birch wood amphiphilic and hydrophilic extractives with retention time, mass-to-charge ratio, compound type annotation and TIC abundance values. (CONTINUED)

| $t_R$ [s] | m/z [Da] | compound type | abundance (peak area) |
|---|---|---|---|
| 284.32 | 325.1092 | Polyphenol | 1327 |
| 286.13 | 261.1345 | Glycerolipid | 1149636 |
| 286.78 | 713.2650 | Phenyl glycoside | 16222 |
| 286.78 | 169.0870 | Fatty Acid and Conjugates | 10076 |
| 287.48 | 201.1131 | Fatty Acid and Conjugates | 29020 |
| 288.37 | 477.2117 | Phenyl glycoside | 89158 |
| 289.40 | 417.2083 | Glycolipid | 515144 |
| 290.29 | 287.1500 | Fatty Acid and Conjugates | 142356 |
| 291.03 | 171.0991 | Fatty Acid and Conjugates | 29738 |
| 291.21 | 523.1855 | Phenyl glycoside | 241697 |
| 291.21 | 524.1882 | Phenyl glycoside | 64695 |
| 291.66 | 327.1233 | Polyphenol | 438358 |
| 291.69 | 489.1955 | Phenyl glycoside | 14071 |
| 292.01 | 189.1132 | Fatty Acid and Conjugates | 311231 |
| 292.72 | 345.2285 | Glycolipid | 12480 |
| 293.01 | 241.1075 | Phenol | 57114 |
| 294.69 | 325.1085 | Polyphenol | 194216 |
| 295.71 | 195.0304 | Phenol | 1861 |
| 295.79 | 505.1331 | Phenyl glycoside | 18476 |
| 296.57 | 507.1846 | Phenyl glycoside | 238919 |
| 298.50 | 583.2065 | Phenyl glycoside | 51378 |
| 298.75 | 525.1611 | Phenyl glycoside | 2580155 |
| 298.76 | 526.1639 | Phenyl glycoside | 655334 |
| 298.79 | 475.2034 | Phenyl glycoside | 1486170 |
| 298.79 | 527.1673 | Phenyl glycoside | 143984 |
| 298.96 | 713.2658 | Phenyl glycoside | 239783 |
| 299.36 | 401.1236 | Polyphenol | 2122 |
| 299.50 | 431.1231 | Polyphenol | 17192 |
| 299.58 | 188.1008 | Fatty Acid and Conjugates | 214550 |
| 299.60 | 187.0981 | Fatty Acid and Conjugates | 2388556 |
| 299.71 | 169.0865 | Fatty Acid and Conjugates | 37009 |
| 300.01 | 209.0791 | Fatty Acid and Conjugates | 18964 |
| 300.30 | 359.1547 | Polyphenol | 22013 |
| 300.40 | 549.2063 | Phenyl glycoside | 12584 |
| 302.53 | 496.1522 | Phenyl glycoside | 63271 |
| 302.68 | 495.1496 | Phenyl glycoside | 252238 |
| 302.78 | 343.2113 | Fatty Acid and Conjugates | 20459 |
| 310.03 | 203.0917 | Fatty Acid and Conjugates | 38487 |
| 310.58 | 145.0871 | Fatty Acid and Conjugates | 799226 |
| 311.44 | 261.1331 | Glycerolipid | 71128 |
| 311.73 | 159.1027 | Fatty Acid and Conjugates | 1040 |
| 314.04 | 201.1136 | Fatty Acid and Conjugates | 7577 |
| 315.03 | 593.2604 | Phenyl glycoside | 44422 |
| 315.09 | 594.2638 | Phenyl glycoside | 15108 |
| 315.11 | 639.2631 | Phenyl glycoside | 35786 |
| 317.00 | 199.0972 | Fatty Acid and Conjugates | 30184 |
| 317.68 | 169.0868 | Fatty Acid and Conjugates | 45778 |
| 320.32 | 325.1100 | Polyphenol | 31468 |
| 322.18 | 553.2180 | Phenyl glycoside | 6508 |

Table SI–5: List of compound features detected via UHPLC-ESI-TOF-MS analysis of birch wood amphiphilic and hydrophilic extractives with retention time, mass-to-charge ratio, compound type annotation and TIC abundance values. (CONTINUED)

| **$t_R$ [s]** | **m/z [Da]** | **compound type** | **abundance (peak area)** |
|---|---|---|---|
| 322.76 | 569.2238 | Phenyl glycoside | 65186 |
| 323.89 | 287.1485 | Fatty Acid and Conjugates | 28267 |
| 323.94 | 345.2270 | Glycolipid | 129213 |
| 324.47 | 159.1026 | Fatty Acid and Conjugates | 105229 |
| 324.75 | 273.1707 | Fatty Acid and Conjugates | 75948 |
| 326.86 | 201.1135 | Fatty Acid and Conjugates | 259524 |
| 330.11 | 433.2055 | Glycolipid | 27952 |
| 335.87 | 583.2153 | Phenyl glycoside | 8839 |
| 336.31 | 171.1028 | Fatty Acid and Conjugates | 470984 |
| 343.27 | 327.2177 | Fatty Acid and Conjugates | 29317 |
| 343.81 | 245.1386 | Fatty Acid and Conjugates | 32307 |
| 345.12 | 301.2021 | Fatty Acid and Conjugates | 17220 |
| 350.27 | 159.1020 | Fatty Acid and Conjugates | 23332 |
| 357.74 | 171.1025 | Fatty Acid and Conjugates | 307768 |
| 358.77 | 273.1698 | Fatty Acid and Conjugates | 5382 |
| 360.39 | 169.0866 | Fatty Acid and Conjugates | 13367 |
| 361.77 | 201.1134 | Fatty Acid and Conjugates | 97369 |
| 362.86 | 331.2382 | Fatty Acid and Conjugates | 47866 |
| 364.73 | 225.1492 | Fatty Acid and Conjugates | 14888 |
| 365.26 | 343.2112 | Fatty Acid and Conjugates | 66047 |
| 366.16 | 329.2329 | Fatty Acid and Conjugates | 2160958 |
| 371.00 | 345.2272 | Glycolipid | 125420 |
| 371.14 | 301.1651 | Fatty Acid and Conjugates | 12121 |
| 380.04 | 331.2474 | Fatty Acid and Conjugates | 82937 |
| 385.14 | 169.0846 | Fatty Acid and Conjugates | 44562 |
| 389.80 | 329.2331 | Fatty Acid and Conjugates | 691429 |
| 394.42 | 301.2007 | Fatty Acid and Conjugates | 7506 |
| 406.27 | 331.2468 | Fatty Acid and Conjugates | 30040 |
| 408.75 | 297.1498 | Polyphenol | 13702 |
| 415.63 | 293.1193 | Polyphenol | 12522 |
| 417.85 | 331.2494 | Fatty Acid and Conjugates | 209142 |
| 419.96 | 207.1380 | Phenol | 2835 |
| 428.08 | 516.3530 | Phospholipid | 17135 |
| 428.99 | 293.1757 | Polyphenol | 15056 |
| 433.64 | 207.1390 | Phenol | 37118 |
| 442.05 | 293.1750 | Polyphenol | 3511 |
| 458.20 | 293.1760 | Polyphenol | 37926 |
| 474.16 | 293.2098 | Fatty Acid and Conjugates | 3713 |
| 517.22 | 293.2100 | Fatty Acid and Conjugates | 6204 |

## Results and Discussion – Chemical Characteristics of Cured Adhesive-Extractives Mixtures

In Figure SI–3, the fingerprint region of FTIR spectra for MUF components and cured adhesive as well as cured and uncured PUR adhesive are shown.

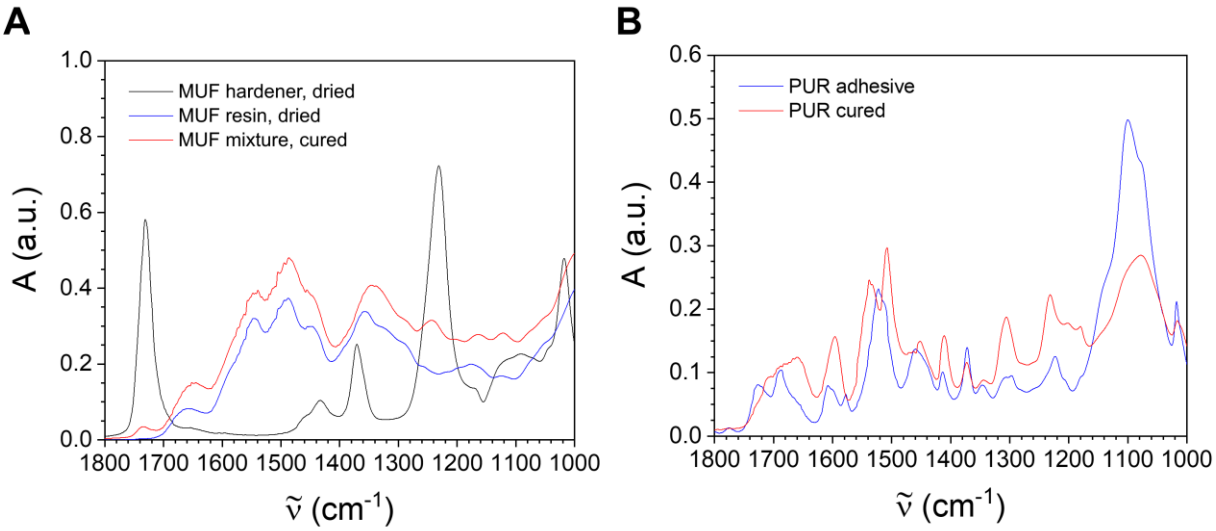


Figure SI–3: FTIR spectra of A) MUF components (dried hardener – black; dried resin – blue) and cured MUF mixture (red) and B) PUR (uncured – blue; cured – red)

**Results and Discussion – Rheological Experiments – Adhesive Curing Behavior**

Experimental data for MUF and PUR curing rheological experiments are shown in the following figures (from Figure SI–4 to Figure SI–19): The progression of the storage modulus (G') and loss modulus (G") at 1 Hz together with the loss modulus peak, indicating glass formation ($t_{glass}$, blue dashed line) and the crossover time when of G' and G" at 1 Hz ($t_{cross}$, brown dashed line), are shown in A. The dynamic viscosity (η*) together with the gel point $t_{\eta}$ – indicated by reaching 100 Pa·s – are shown in B. The loss factor (tan δ) is shown for the lowest frequency (1 Hz), highest frequency (10 Hz) and the geometric mean (√10 Hz) in C, together with the time of crossover at the respective frequencies (dashed lines). In D, the progression of the frequency-dependent variance of the loss factor (tan δ) and its local minimum ($t_{gel}$, violet dashed line), indicating percolation and, thus, the occurrence of the gelation, is shown, which is also marked in C (empty violet circle).

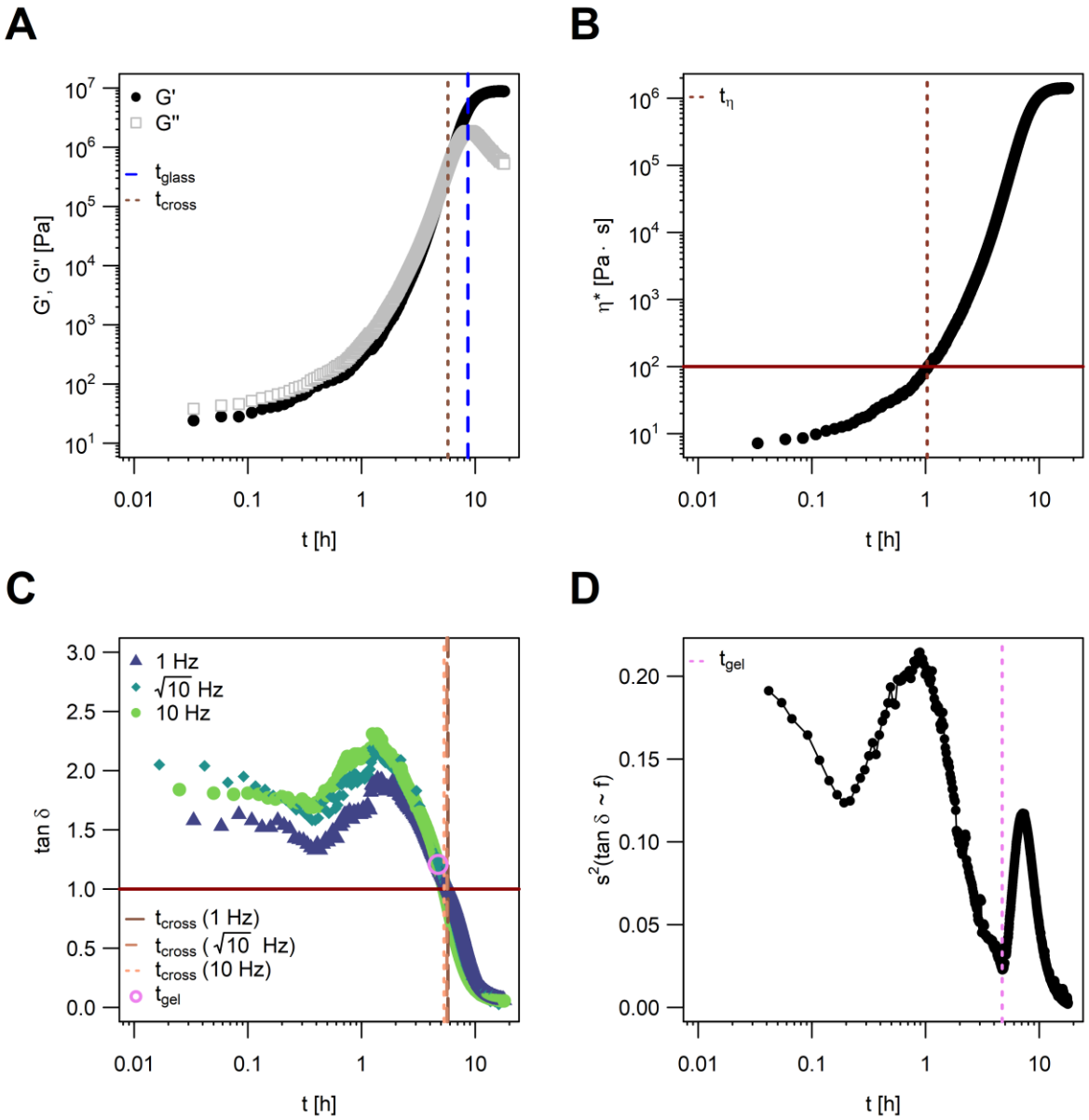


Figure SI–4: Isothermal time-sweep experiment at 20 °C/65%-RH during the curing process of MUF adhesive without extractives addition on pristine birch wood: A) storage modulus G' and loss modulus G" at 1 Hz – the blue dashed line corresponds to the vitrification time tglass and the brown dashed to the crossover time tcross (tan δ = 1) -; B) dynamic viscosity η* at 1 Hz – the dashed line corresponds to the gel point tη-; C) loss factor tan δ with at different frequency values – the dashed lines correspond to the crossover time tcross (tan δ = 1) and violet circle to the gel time tgel-; and D) loss factor variance – the dashed line corresponds to the local minimum variance indicating gel time tgel.

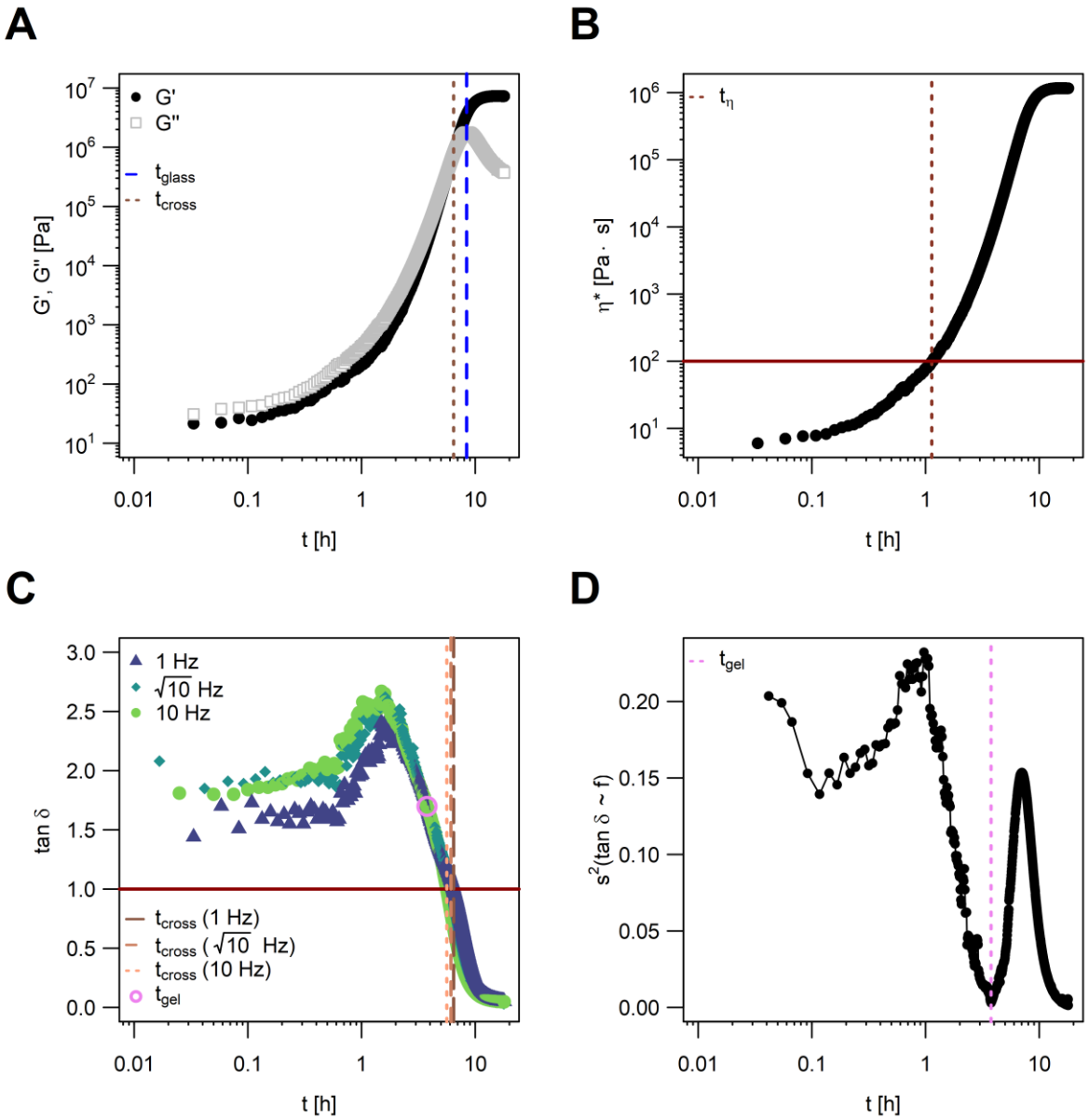


Figure SI–5: Isothermal time-sweep experiment at 20 °C/65%-RH during the curing process of MUF adhesive without extractives addition on extracted birch wood: A) storage modulus G' and loss modulus G" at 1 Hz – the blue dashed line corresponds to the vitrification time tglass and the brown dashed to the crossover time tcross (tan δ = 1) -; B) dynamic viscosity η* at 1 Hz – the dashed line corresponds to the gel point tη-; C) loss factor tan δ with at different frequency values – the dashed lines correspond to the crossover time tcross (tan δ = 1) and violet circle to the gel time tgel-; and D) loss factor variance – the dashed line corresponds to the local minimum variance indicating gel time tgel.

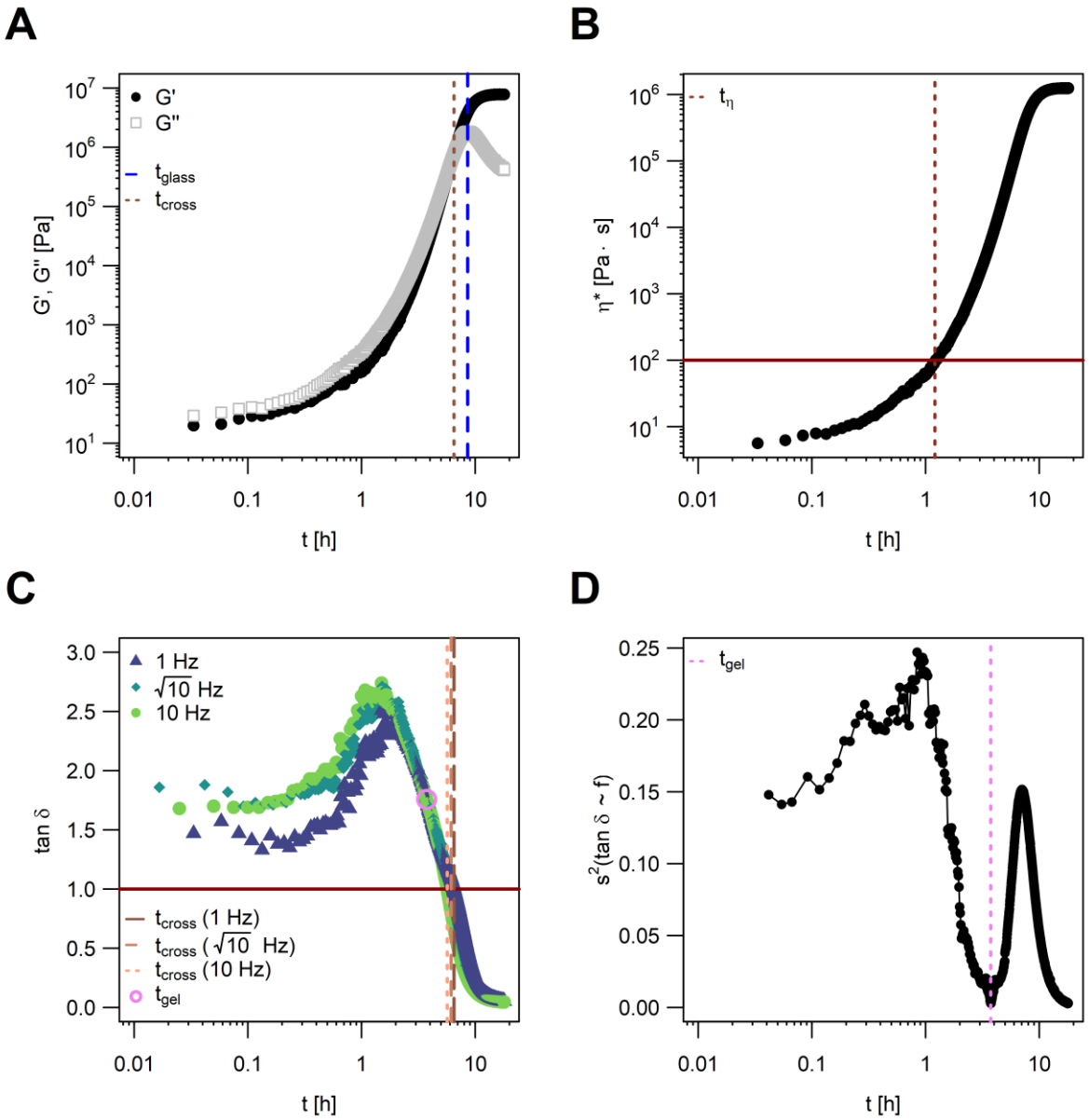


Figure SI–6: Isothermal time-sweep experiment at 20 °C/65% RH during the curing process of MUF adhesive with added extractive concentration of 0.2% (W/W) on extracted birch wood: A) storage modulus G' and loss modulus G" at 1 Hz – the blue dashed line corresponds to the vitrification time $t_{glass}$ and the brown dashed to the crossover time $t_{cross}$ (tan δ = 1) -; B) dynamic viscosity η* at 1 Hz – the dashed line corresponds to the gel point $t_\eta$-; C) loss factor tan δ with at different frequency values – the dashed lines correspond to the crossover time $t_{cross}$ (tan δ = 1) and violet circle to the gel time $t_{gel}$-; and D) loss factor variance – the dashed line corresponds to the local minimum variance indicating gel time $t_{gel}$.

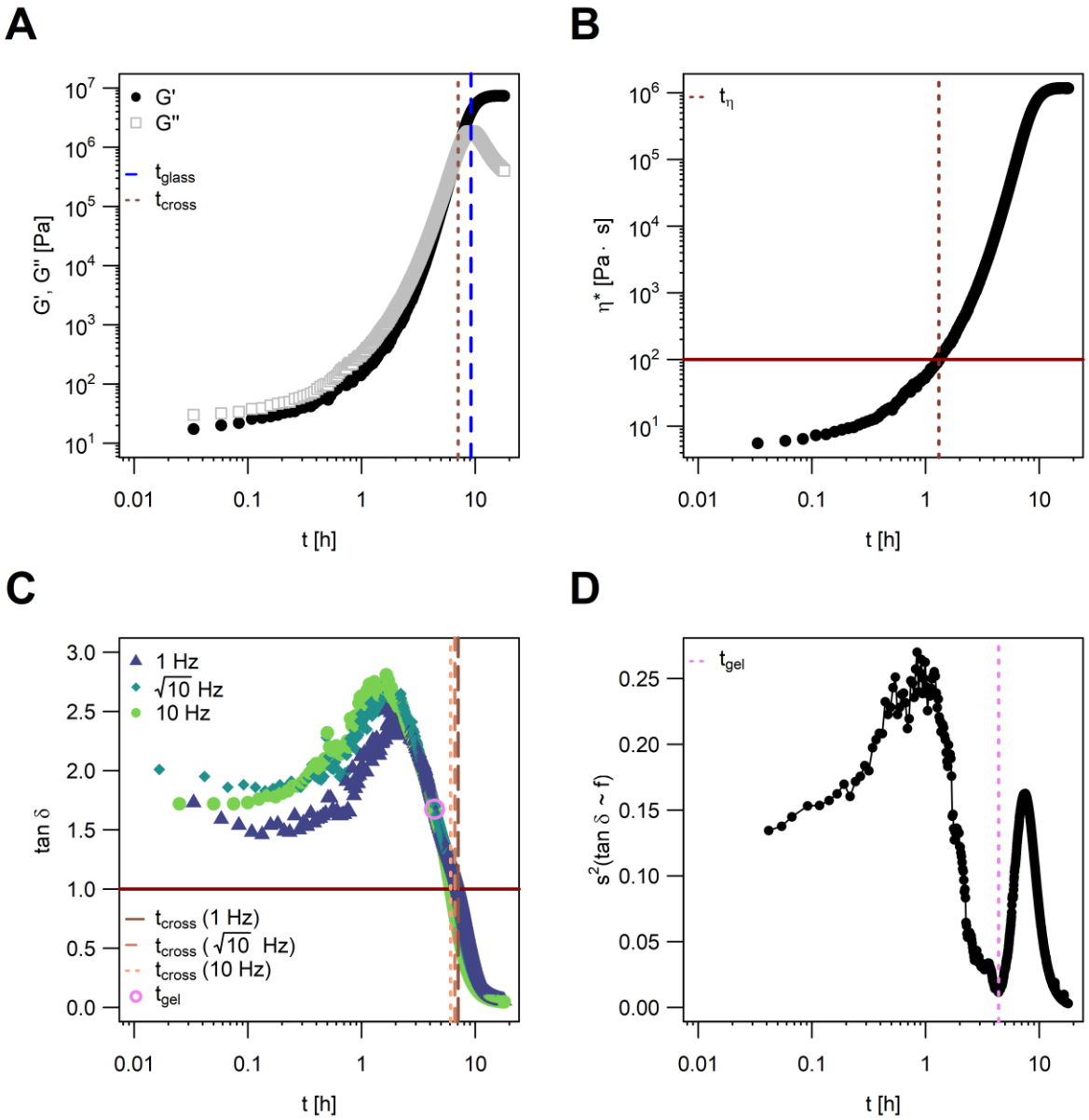


Figure SI–7: Isothermal time-sweep experiment at 20 °C/65% RH during the curing process of MUF adhesive with added extractive concentration of 0.4% (W/W) on extracted birch wood: A) storage modulus G' and loss modulus G" at 1 Hz – the blue dashed line corresponds to the vitrification time $t_{glass}$ and the brown dashed to the crossover time $t_{cross}$ (tan δ = 1) -; B) dynamic viscosity η* at 1 Hz – the dashed line corresponds to the gel point $t_\eta$-; C) loss factor tan δ with at different frequency values – the dashed lines correspond to the crossover time $t_{cross}$ (tan δ = 1) and violet circle to the gel time $t_{gel}$-; and D) loss factor variance – the dashed line corresponds to the local minimum variance indicating gel time $t_{gel}$.

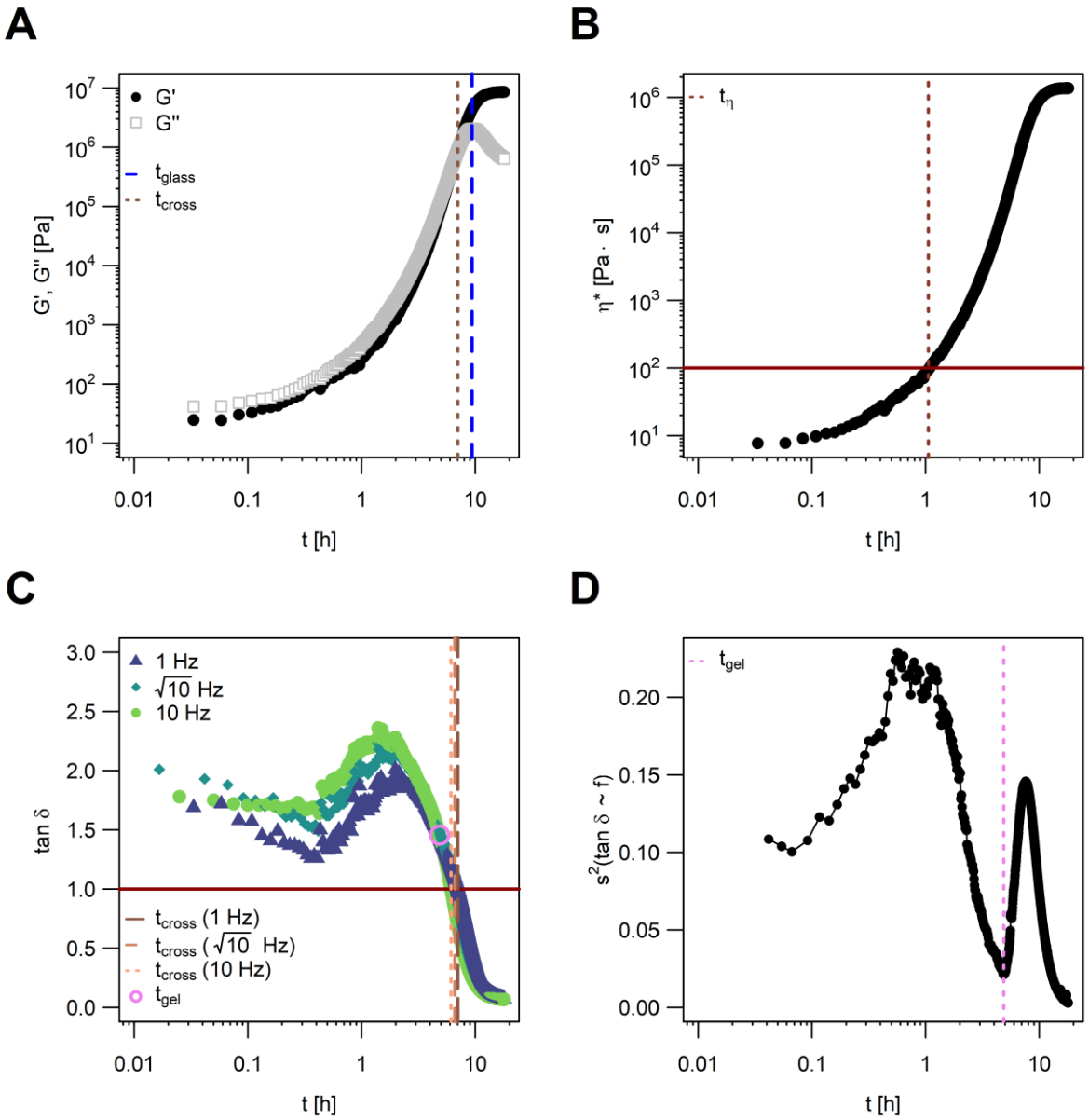


Figure SI–8: Isothermal time-sweep experiment at 20 °C/65% RH during the curing process of MUF adhesive with added extractive concentration of 0.6% (W/W) on extracted birch wood: A) storage modulus G' and loss modulus G" at 1 Hz – the blue dashed line corresponds to the vitrification time $t_{glass}$ and the brown dashed to the crossover time $t_{cross}$ (tan δ = 1) -; B) dynamic viscosity η* at 1 Hz – the dashed line corresponds to the gel point $t_\eta$-; C) loss factor tan δ with at different frequency values – the dashed lines correspond to the crossover time $t_{cross}$ (tan δ = 1) and violet circle to the gel time $t_{gel}$-; and D) loss factor variance – the dashed line corresponds to the local minimum variance indicating gel time $t_{gel}$.

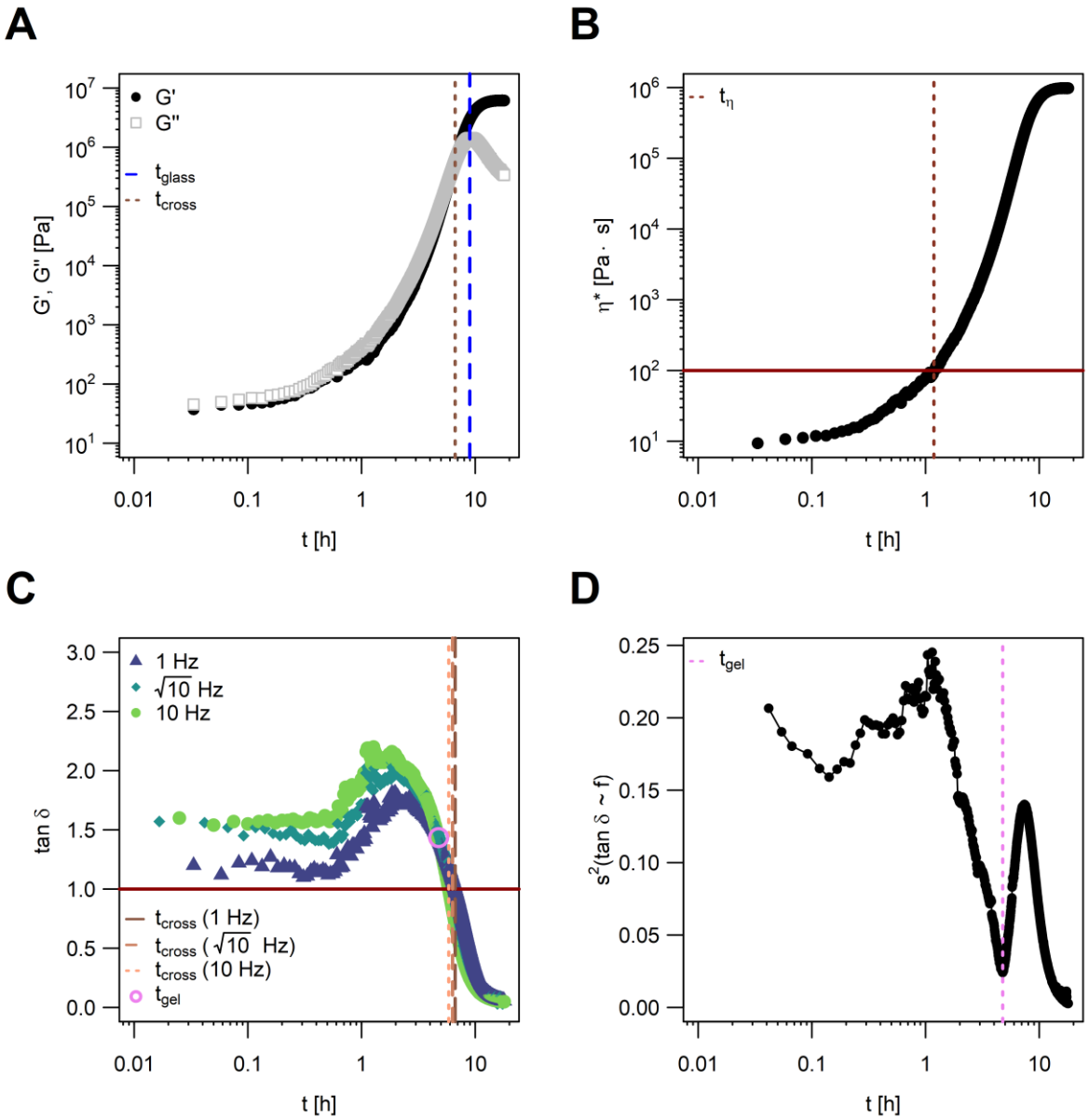


Figure SI–9: Isothermal time-sweep experiment at 20 °C/65% RH during the curing process of MUF adhesive with added extractive concentration of 0.8% (W/W) on extracted birch wood: A) storage modulus G' and loss modulus G" at 1 Hz – the blue dashed line corresponds to the vitrification time $t_{glass}$ and the brown dashed to the crossover time $t_{cross}$ (tan δ = 1) -; B) dynamic viscosity η* at 1 Hz – the dashed line corresponds to the gel point $t_\eta$-; C) loss factor tan δ with at different frequency values – the dashed lines correspond to the crossover time $t_{cross}$ (tan δ = 1) and violet circle to the gel time $t_{gel}$-; and D) loss factor variance – the dashed line corresponds to the local minimum variance indicating gel time $t_{gel}$.

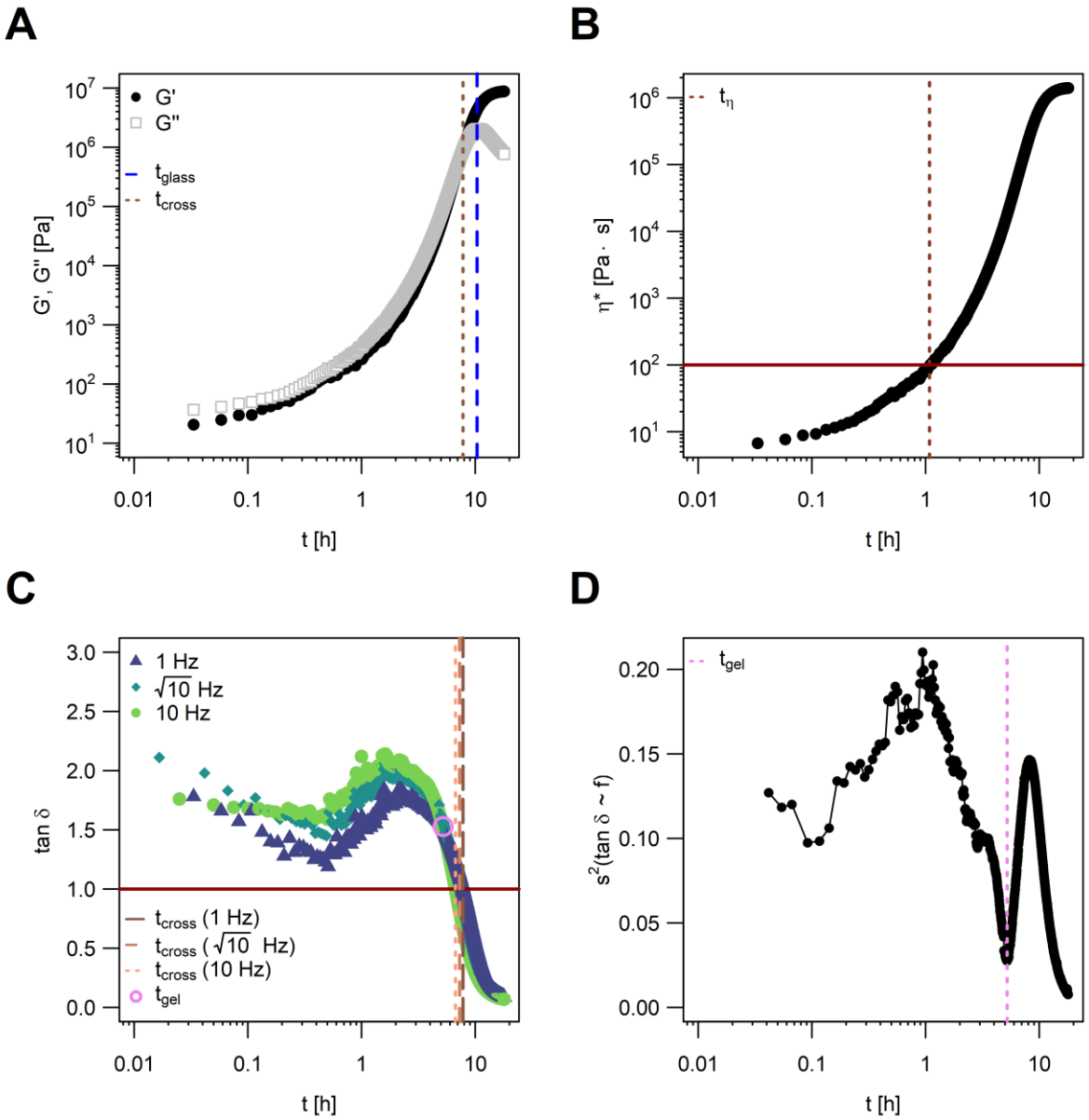


Figure SI–10: Isothermal time-sweep experiment at 20 °C/65% RH during the curing process of MUF adhesive with added extractive concentration of 1.0% (W/W) on extracted birch wood: A) storage modulus G' and loss modulus G" at 1 Hz – the blue dashed line corresponds to the vitrification time $t_{glass}$ and the brown dashed to the crossover time $t_{cross}$ (tan δ = 1) -; B) dynamic viscosity η* at 1 Hz – the dashed line corresponds to the gel point $t_\eta$-; C) loss factor tan δ with at different frequency values – the dashed lines correspond to the crossover time $t_{cross}$ (tan δ = 1) and violet circle to the gel time $t_{gel}$-; and D) loss factor variance – the dashed line corresponds to the local minimum variance indicating gel time $t_{gel}$.

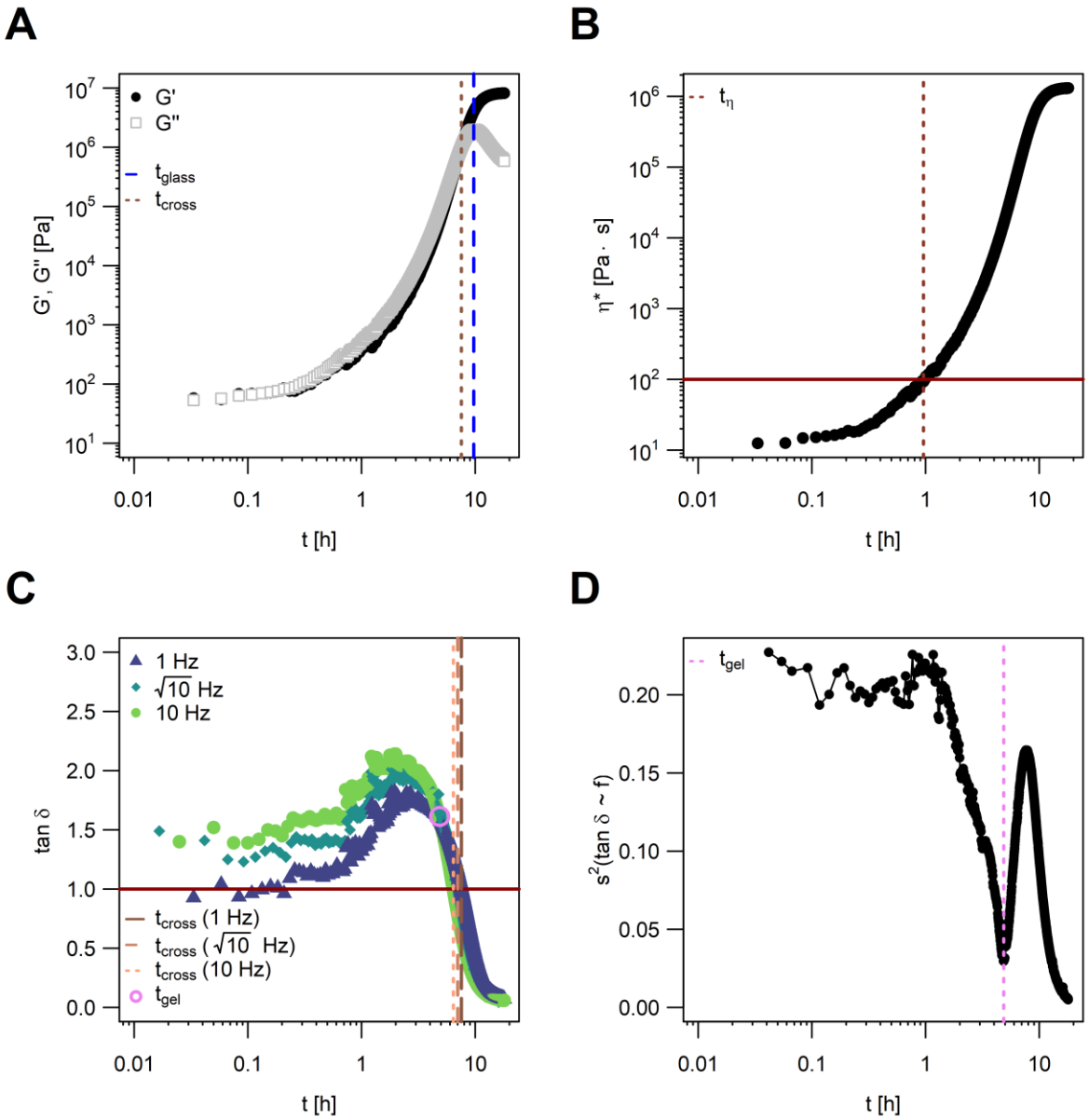


Figure SI–11: Isothermal time-sweep experiment at 20 °C/65% RH during the curing process of MUF adhesive with added extractive concentration of 1.2% (W/W) on extracted birch wood: A) storage modulus G' and loss modulus G" at 1 Hz – the blue dashed line corresponds to the vitrification time $t_{glass}$ and the brown dashed to the crossover time $t_{cross}$ (tan δ = 1) -; B) dynamic viscosity η* at 1 Hz – the dashed line corresponds to the gel point $t_\eta$-; C) loss factor tan δ with at different frequency values – the dashed lines correspond to the crossover time $t_{cross}$ (tan δ = 1) and violet circle to the gel time $t_{gel}$-; and D) loss factor variance – the dashed line corresponds to the local minimum variance indicating gel time $t_{gel}$.

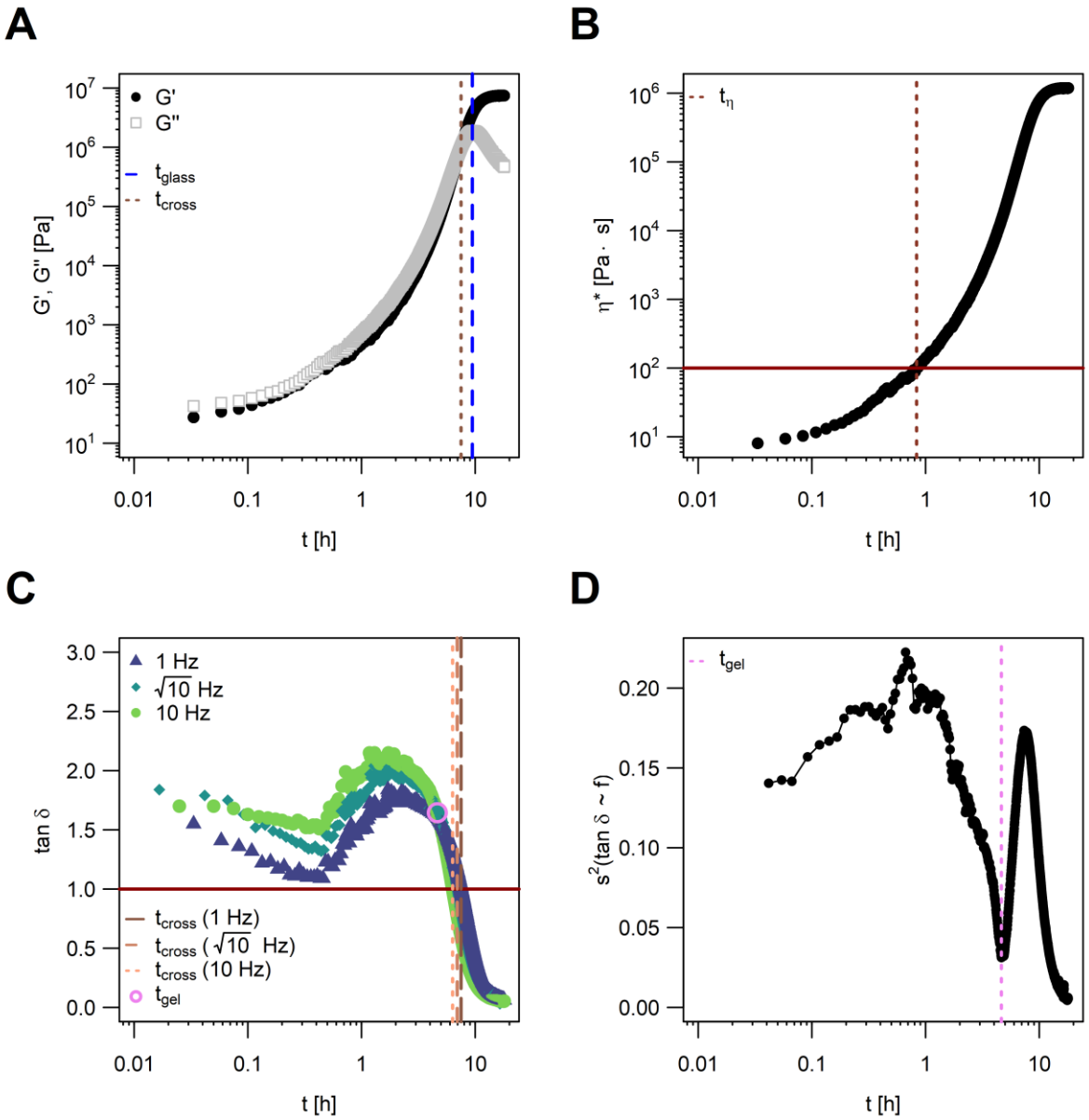


Figure SI–12: Isothermal time-sweep experiment at 20 °C/65% RH during the curing process of MUF adhesive with added extractive concentration of 1.4% (W/W) on extracted birch wood: A) storage modulus G' and loss modulus G" at 1 Hz – the blue dashed line corresponds to the vitrification time $t_{glass}$ and the brown dashed to the crossover time $t_{cross}$ (tan δ = 1) -; B) dynamic viscosity η* at 1 Hz – the dashed line corresponds to the gel point $t_\eta$-; C) loss factor tan δ with at different frequency values – the dashed lines correspond to the crossover time $t_{cross}$ (tan δ = 1) and violet circle to the gel time $t_{gel}$-; and D) loss factor variance – the dashed line corresponds to the local minimum variance indicating gel time $t_{gel}$.

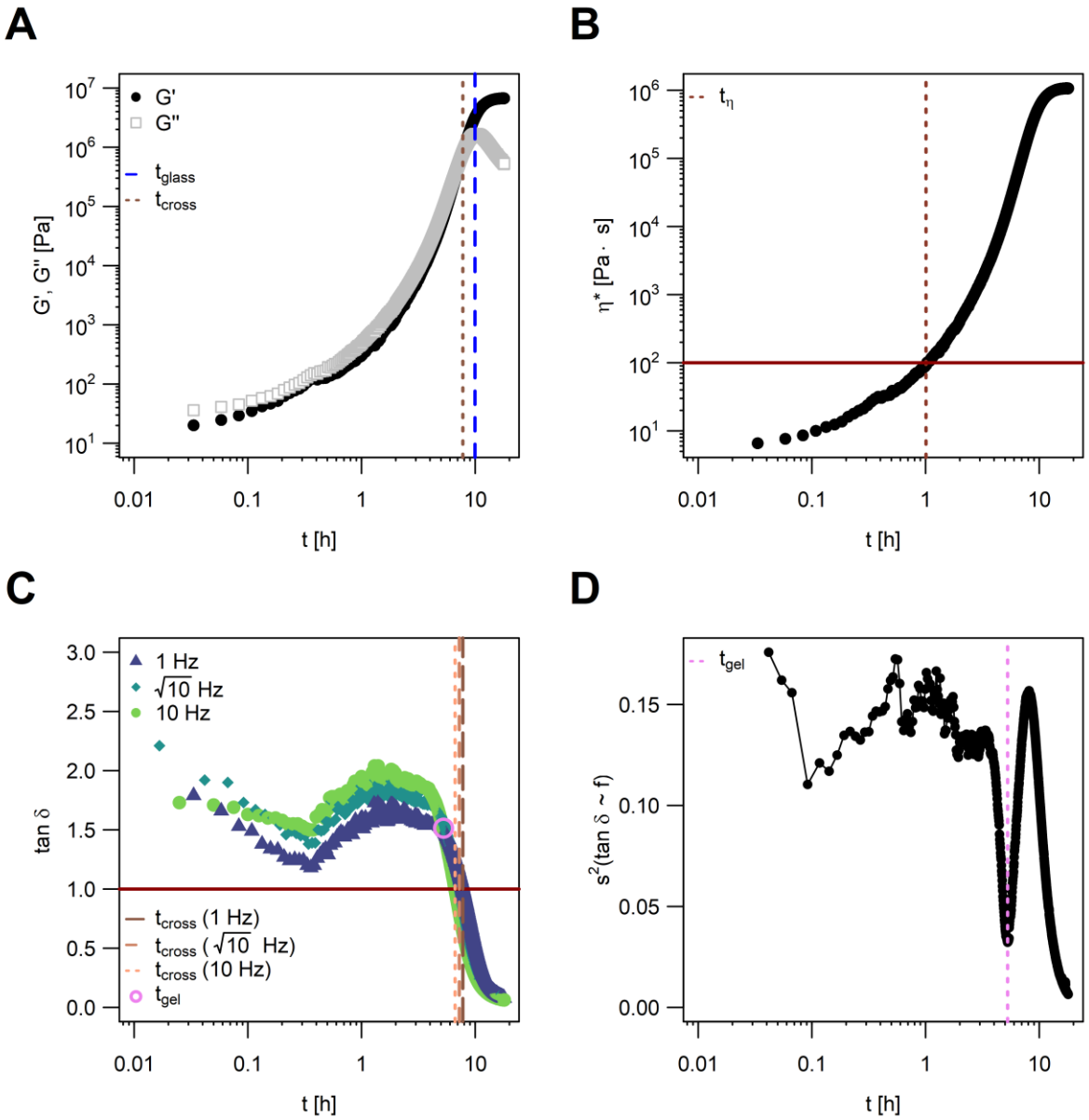


Figure SI–13: Isothermal time-sweep experiment at 20 °C/65% RH during the curing process of MUF adhesive with added extractive concentration of 1.6% (W/W) on extracted birch wood: A) storage modulus G' and loss modulus G" at 1 Hz – the blue dashed line corresponds to the vitrification time $t_{glass}$ and the brown dashed to the crossover time $t_{cross}$ (tan δ = 1) -; B) dynamic viscosity η* at 1 Hz – the dashed line corresponds to the gel point $t_\eta$-; C) loss factor tan δ with at different frequency values – the dashed lines correspond to the crossover time $t_{cross}$ (tan δ = 1) and violet circle to the gel time $t_{gel}$-; and D) loss factor variance – the dashed line corresponds to the local minimum variance indicating gel time $t_{gel}$.

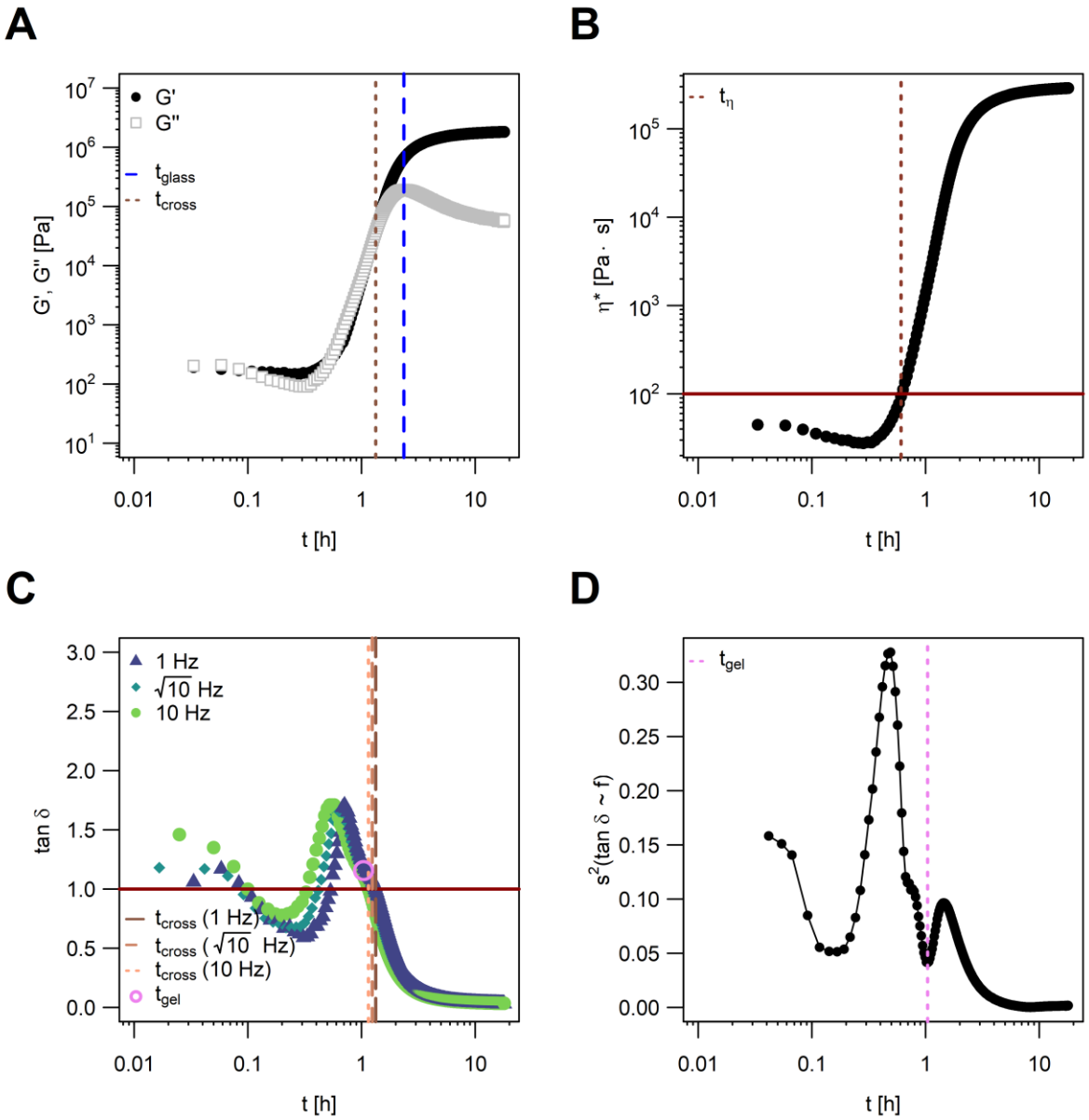


Figure SI–14: Isothermal time-sweep experiment at 20 °C/65%-RH during the curing process of PUR adhesive without extractives addition on pristine birch wood: A) storage modulus G' and loss modulus G" at 1 Hz – the blue dashed line corresponds to the vitrification time $t_{glass}$ and the brown dashed to the crossover time $t_{cross}$ (tan δ = 1) -; B) dynamic viscosity η* at 1 Hz – the dashed line corresponds to the gel point $t_\eta$-; C) loss factor tan δ with at different frequency values – the dashed lines correspond to the crossover time $t_{cross}$ (tan δ = 1) and violet circle to the gel time $t_{gel}$-; and D) loss factor variance – the dashed line corresponds to the local minimum variance indicating gel time $t_{gel}$.

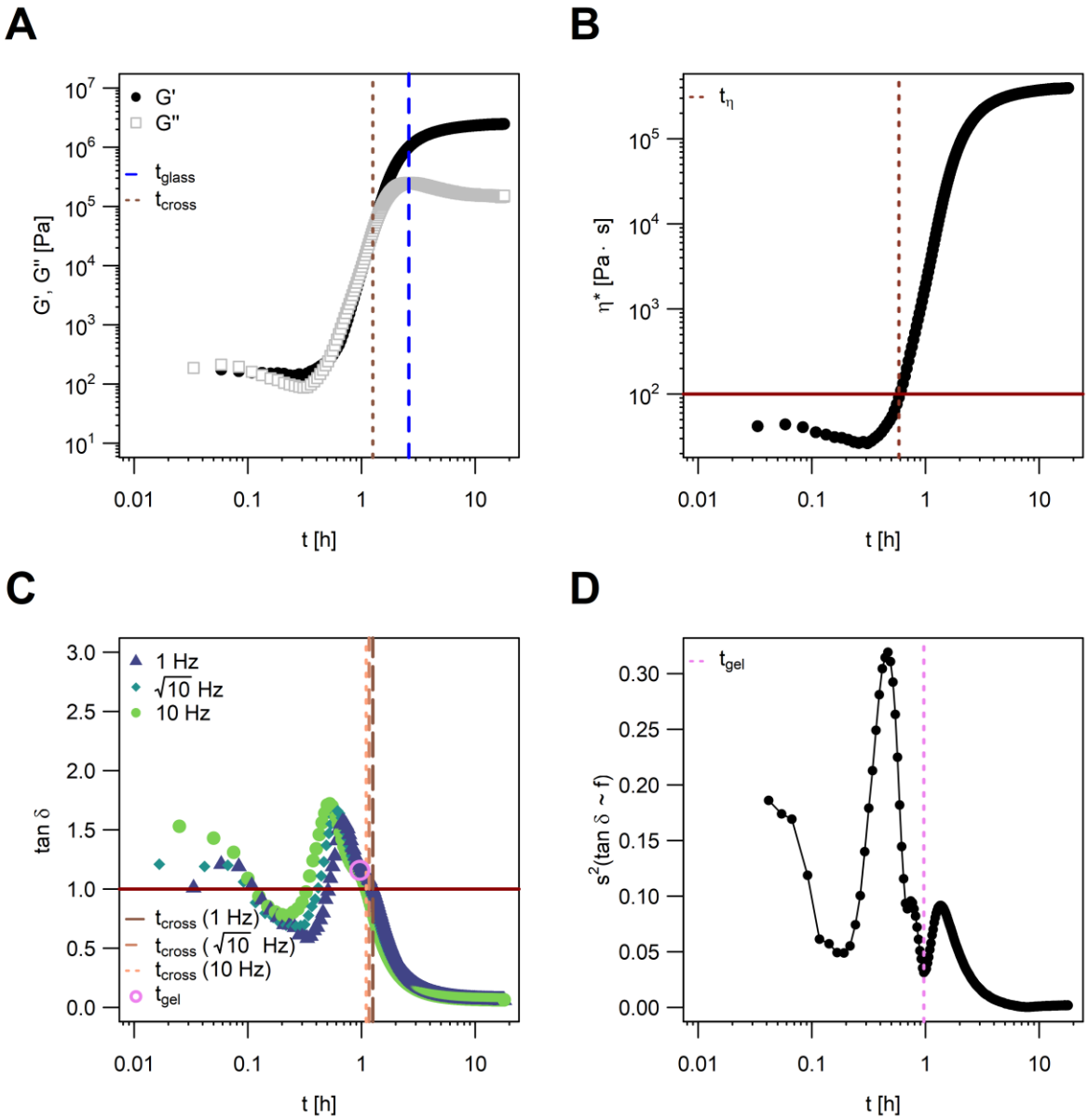


Figure SI–15: Isothermal time-sweep experiment at 20 °C/65%-RH during the curing process of PUR adhesive without extractives addition on extracted birch wood: A) storage modulus G' and loss modulus G" at 1 Hz – the blue dashed line corresponds to the vitrification time $t_{glass}$ and the brown dashed to the crossover time $t_{cross}$ (tan δ = 1) -; B) dynamic viscosity η* at 1 Hz – the dashed line corresponds to the gel point $t_\eta$-; C) loss factor tan δ with at different frequency values – the dashed lines correspond to the crossover time $t_{cross}$ (tan δ = 1) and violet circle to the gel time $t_{gel}$-; and D) loss factor variance – the dashed line corresponds to the local minimum variance indicating gel time $t_{gel}$.

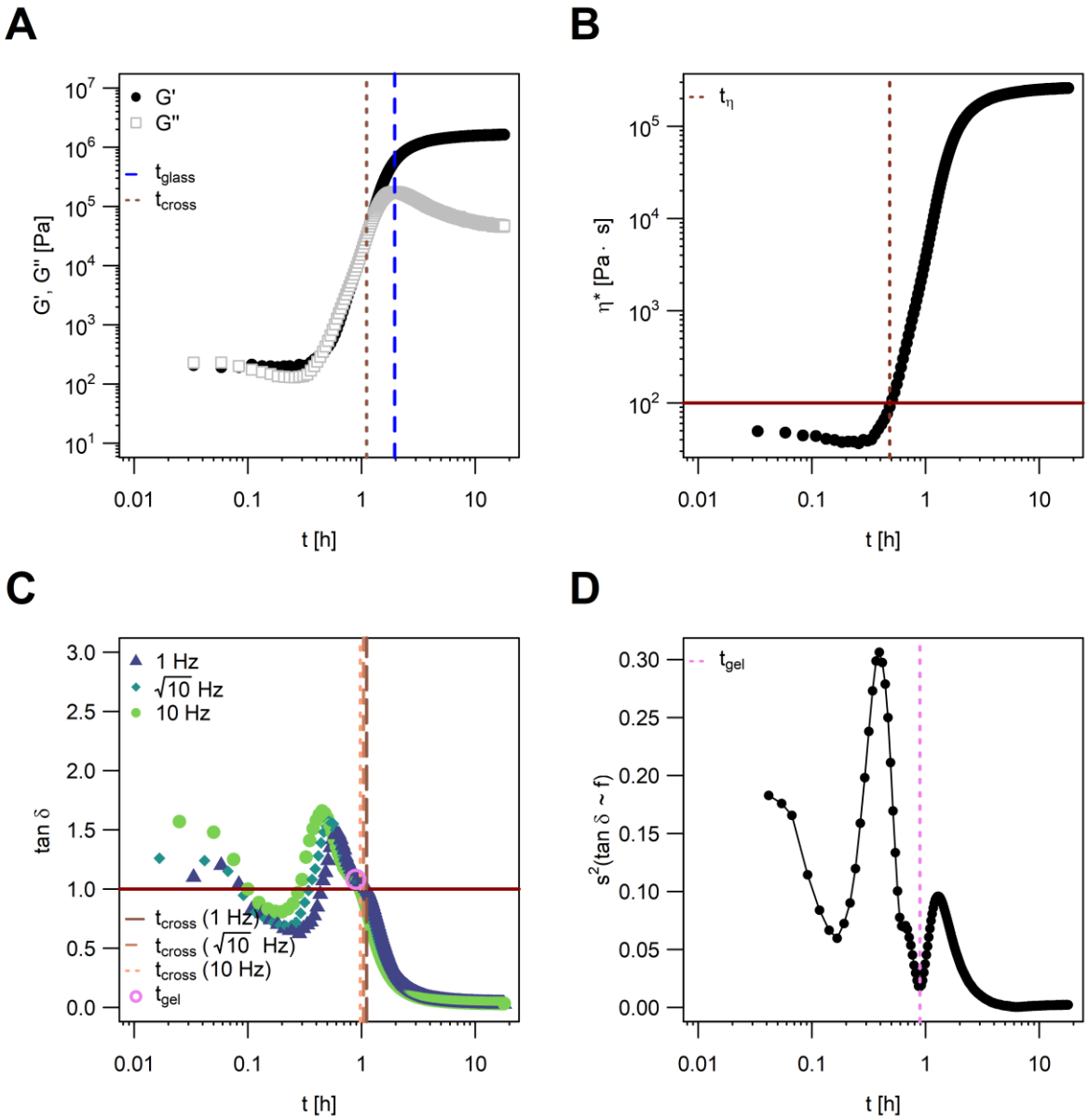


Figure SI–16: Isothermal time-sweep experiment at 20 °C/65% RH during the curing process of PUR adhesive with added extractive concentration of 0.05% (W/W) on extracted birch wood: A) storage modulus G' and loss modulus G" at 1 Hz – the blue dashed line corresponds to the vitrification time $t_{glass}$ and the brown dashed to the crossover time $t_{cross}$ (tan δ = 1) -; B) dynamic viscosity η* at 1 Hz – the dashed line corresponds to the gel point $t_\eta$-; C) loss factor tan δ with at different frequency values – the dashed lines correspond to the crossover time $t_{cross}$ (tan δ = 1) and violet circle to the gel time $t_{gel}$-; and D) loss factor variance – the dashed line corresponds to the local minimum variance indicating gel time $t_{gel}$.

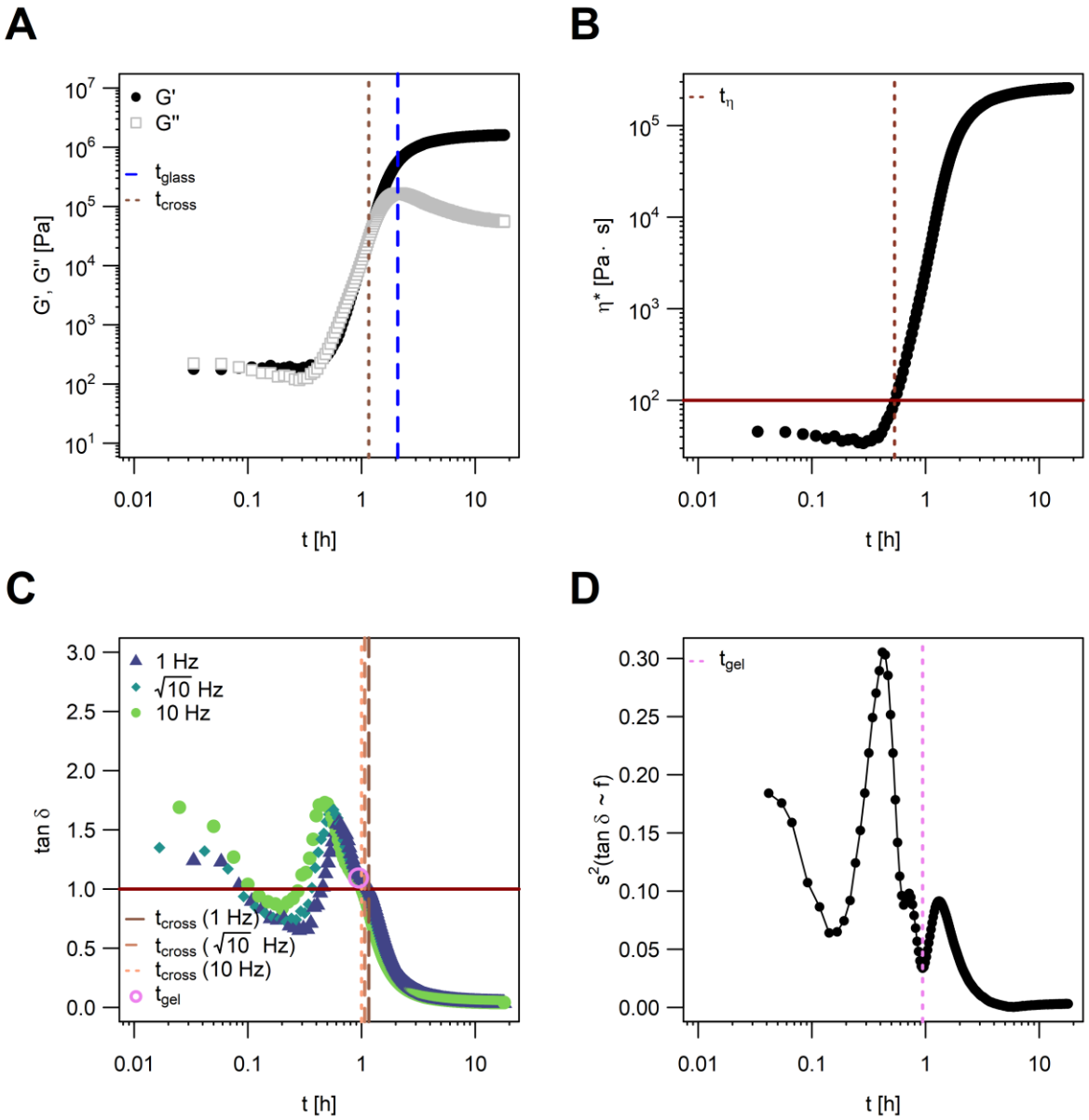


Figure SI–17: Isothermal time-sweep experiment at 20 °C/65% RH during the curing process of PUR adhesive with added extractive concentration of 0.1% (W/W) on extracted birch wood: A) storage modulus G' and loss modulus G" at 1 Hz – the blue dashed line corresponds to the vitrification time $t_{glass}$ and the brown dashed to the crossover time $t_{cross}$ (tan δ = 1) -; B) dynamic viscosity η* at 1 Hz – the dashed line corresponds to the gel point $t_\eta$-; C) loss factor tan δ with at different frequency values – the dashed lines correspond to the crossover time $t_{cross}$ (tan δ = 1) and violet circle to the gel time $t_{gel}$-; and D) loss factor variance – the dashed line corresponds to the local minimum variance indicating gel time $t_{gel}$.

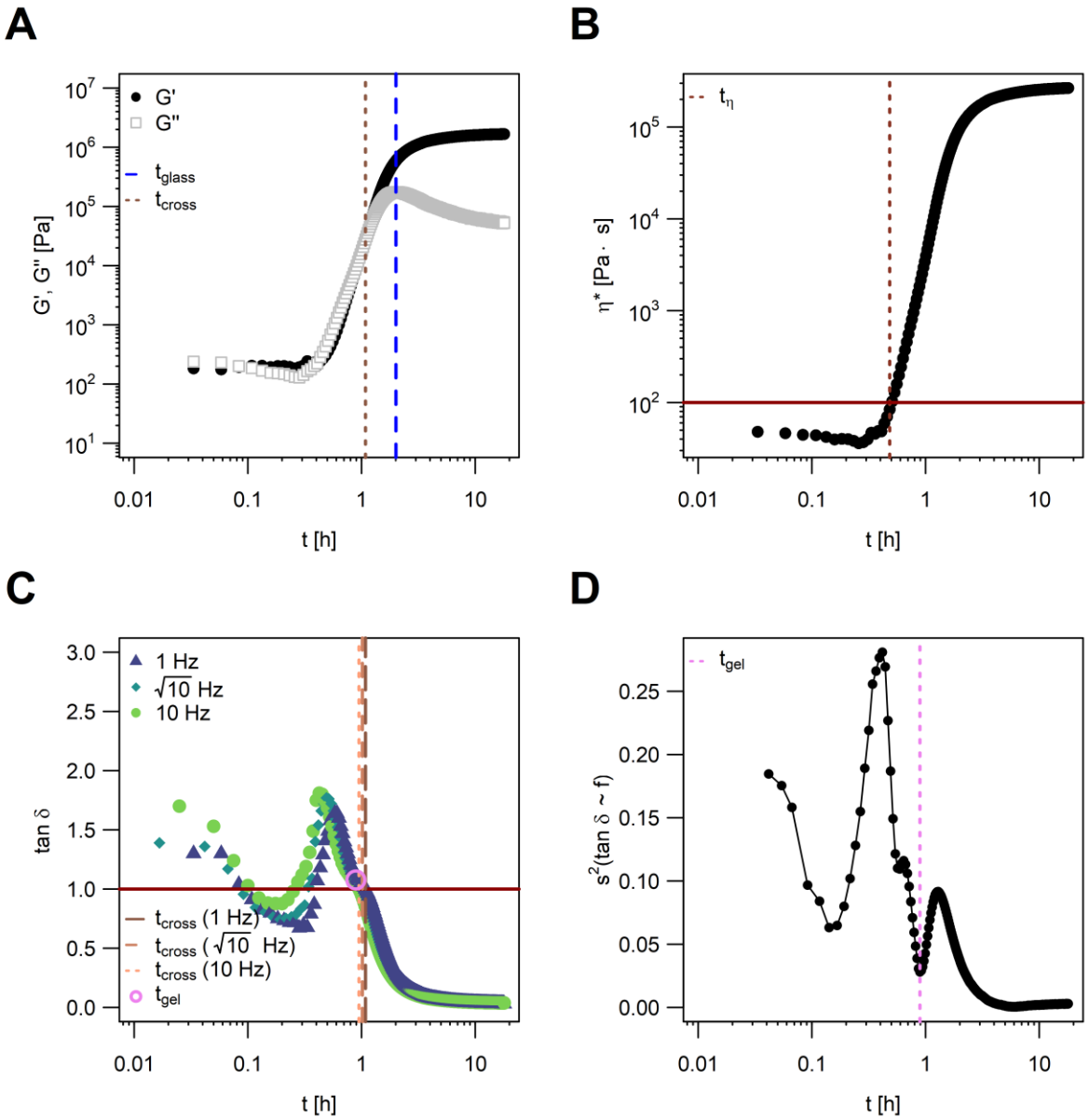


Figure SI–18: Isothermal time-sweep experiment at 20 °C/65% RH during the curing process of PUR adhesive with added extractive concentration of 0.2% (W/W) on extracted birch wood: A) storage modulus G' and loss modulus G" at 1 Hz – the blue dashed line corresponds to the vitrification time $t_{glass}$ and the brown dashed to the crossover time $t_{cross}$ (tan δ = 1) -; B) dynamic viscosity η* at 1 Hz – the dashed line corresponds to the gel point $t_\eta$-; C) loss factor tan δ with at different frequency values – the dashed lines correspond to the crossover time $t_{cross}$ (tan δ = 1) and violet circle to the gel time $t_{gel}$-; and D) loss factor variance – the dashed line corresponds to the local minimum variance indicating gel time $t_{gel}$.

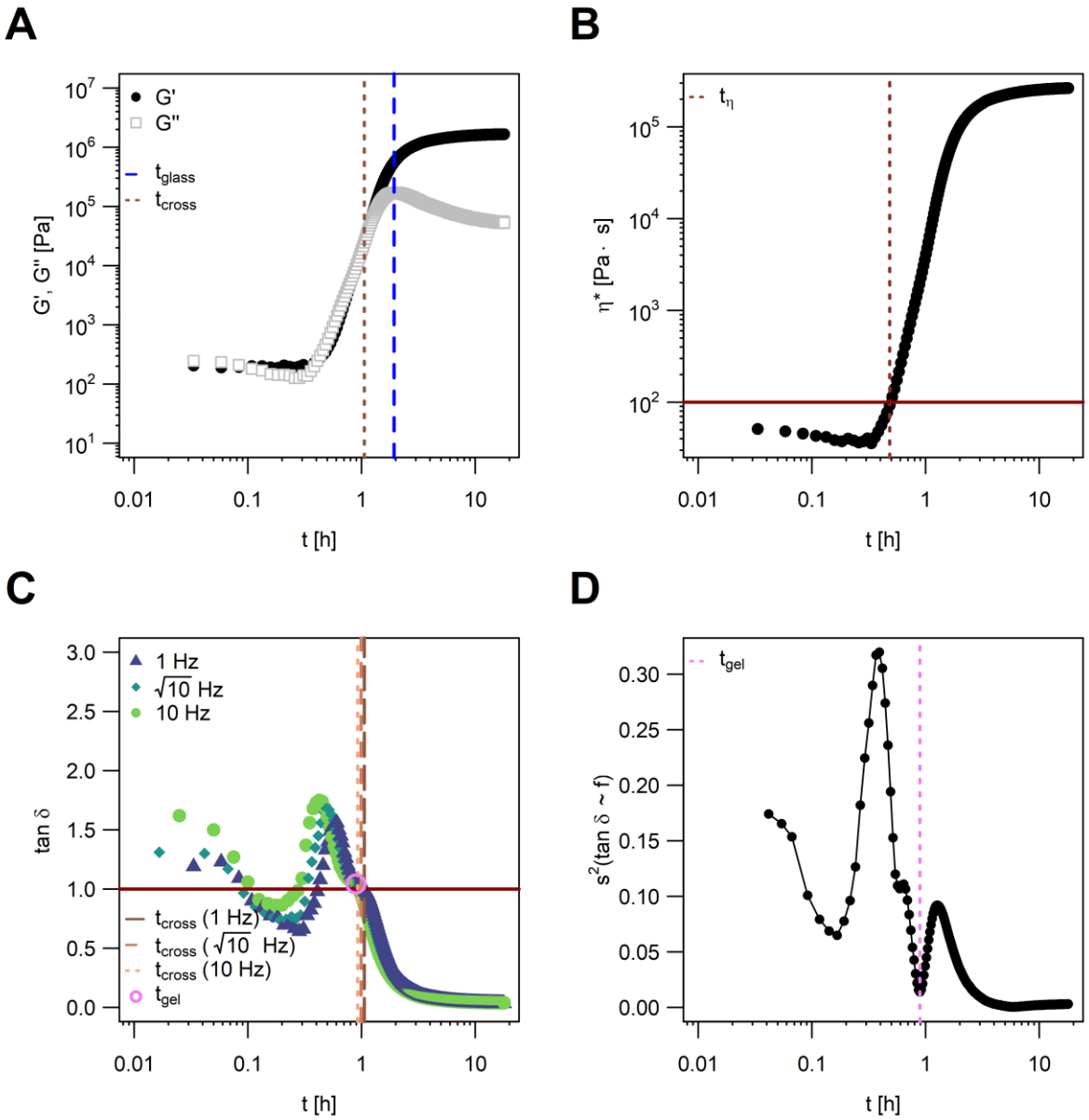


Figure SI–19: Isothermal time-sweep experiment at 20 °C/65% RH during the curing process of PUR adhesive with added extractive concentration of 0.4% (W/W) on extracted birch wood: A) storage modulus G' and loss modulus G" at 1 Hz – the blue dashed line corresponds to the vitrification time $t_{glass}$ and the brown dashed to the crossover time $t_{cross}$ (tan δ = 1) -; B) dynamic viscosity η* at 1 Hz – the dashed line corresponds to the gel point $t_\eta$-; C) loss factor tan δ with at different frequency values – the dashed lines correspond to the crossover time $t_{cross}$ (tan δ = 1) and violet circle to the gel time $t_{gel}$-; and D) loss factor variance – the dashed line corresponds to the local minimum variance indicating gel time $t_{gel}$.

In Figure SI–20A, the progression of the rheometer gap size (adhesive layer thickness, d) throughout the MUF curing experiments on pristine and extracted wood is shown. The thick lines are average curves, and the light curves show the original experimental data. In Figure SI–20B, the progression of the axial pressure in the initial phase of PUR curing experiments due to $CO_2$ development on pristine and extracted wood is shown.

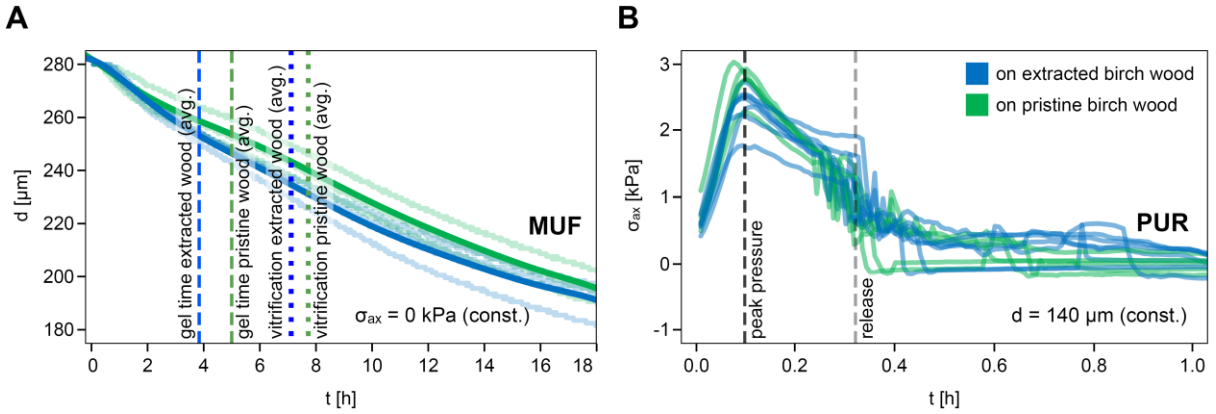


Figure SI–20: A: Progression of the rheometer gap size (adhesive layer thickness, d) throughout the MUF curing experiments on pristine wood (in green, n = 4) and extracted wood (blue, n = 4). The thick lines are average curves, and the light curves show the original experimental data. B: Progression of the axial pressure in the initial phase of PUR curing experiments due to $CO_2$ development on pristine wood (in green, n = 5) and extracted wood (blue, n = 7).

## Results and Discussion – Mechanical Characteristics of Cured Adhesive Films

The stress-strain curves of the performed uniaxial tensile stress-strain (UTSS) measurements on MUF (A and C) and PUR (B and D) adhesive curves with varying concentrations of extractives are shown in Figure SI–21. The color of the respective curves is mapped to extractives concentration as shown as scales in (A) for MUF (0 to 1.0% (W/W)) and in (B) for PUR (0 to 0.2% (W/W)).

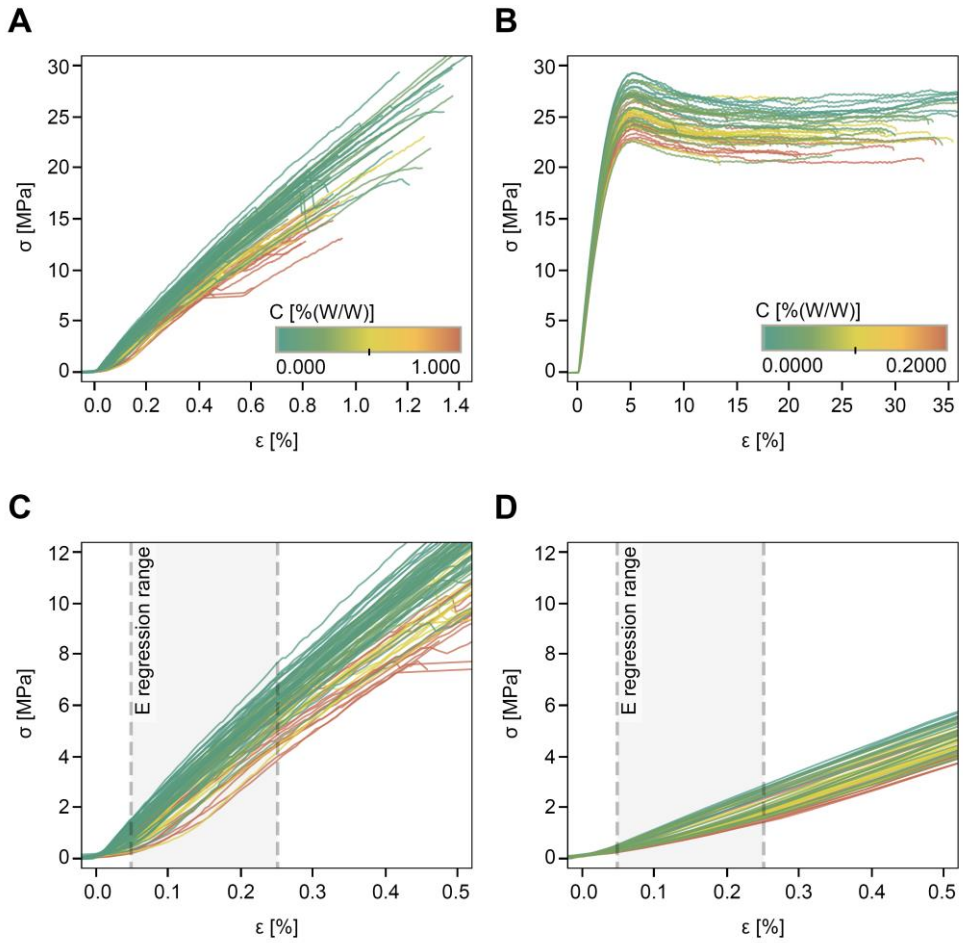


Figure SI–21: Uniaxial tensile stress-strain (UTSS) curves for MUF (A and C) and PUR (B and D) adhesive films. A and B show the complete curves, while C and D show low strain range with the moduli of elasticity regression interval ($0.05 < \varepsilon < 0.25$, as defined in ISO 527–1) in grey. The color of the respective curves is mapped to extractives concentration as shown as scales for (A) MUF and (B) PUR.

The glass transition temperatures $T_g$ as given by TMA measurement and the mid-point evaluation method are shown in Figure SI–22. A polynomial fit with 95% confidence band is shown as a guide to the eyes.

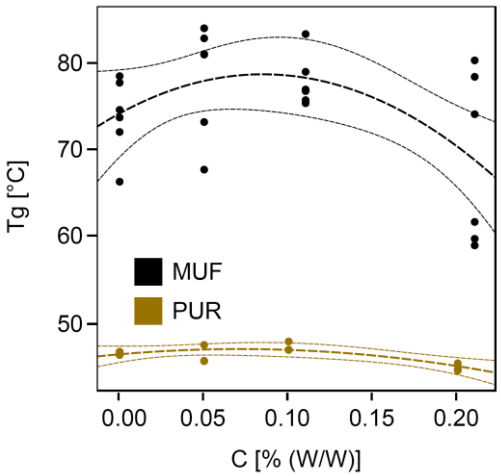


Figure SI–22: Glass transition temperature $T_g$ determined by the mid-point method for adhesive films with increased extractives concentration. Dashed lines show the 2nd-degree polynomial fit with 95% confidence band as a guide to the eyes.

The temperature- and frequency-sweep performed via Dynamic Mechanical Analysis (DMA) on PUR and MUF are shown in Figure SI–23 below. The frequency-sweep was performed at equilibrium climate conditions of 0%-RH, 65%-RH and 90%-RH. Although the MUF is expected to have a higher sorptive moisture content at the respective RH, the effects on the storage modulus E' are smaller than in the case of PUR, since the highly cross-linked it less plasticizable.

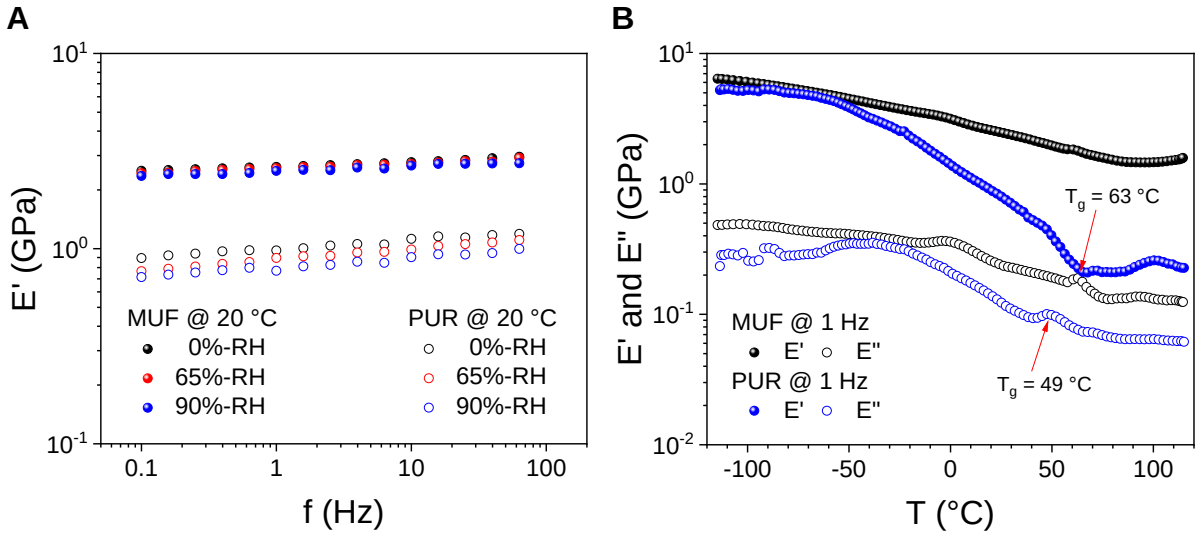


Figure SI–23: Dynamic Mechanical Analysis (DMA) experiments on MUF and PUR adhesive films: A) frequency-sweep experiments at 20 °C and different RH-values; and B) temperature-sweep experiments at 1 Hz and 0%-RH. The glass transition temperature (Tg) is indicated by the peak in the E'' profile.

## Results and Discussion – Tensile Shear Strength Experiments

The statistics of the TSS results, the average change in TSS comparing extracted specimens to pristine wood specimens, and the p-value of ANOVA are shown in Table SI–6.

Table SI–6: Tensile shear strength (TSS) measurements using pristine and extracted birch wood: result statistics.

| **specimen group: adhesive and treatment** | | **tensile shear strength (TSS) average ± standard deviation [MPa]** | | **rel. change in avg. TSS [%]** | **ANOVA: p-value** |
|---|---|---|---|---|---|
| | | **pristine wood** | **extracted wood** | | |
| **PUR** | **A1** | 12.5 ± 2.8 | 11.3 ± 1.7 | +11% | 0.13 |
| | **A2** | 7 ± 2.4 | 6.8 ± 1.7 | +3% | 0.80 |
| | **A4** | 6.2 ± 2.1 | 6.3 ± 1.0 | -2% | 0.81 |
| | **A5** | 11.7 ± 2.1 | 11.4 ± 2.0 | +2% | 0.72 |
| **MUF** | **A1** | 10.7 ± 1.7 | 9.6 ± 1.0 | +11% | 0.026 |
| | **A2** | 8.2 ± 1.5 | 6.7 ± 1.3 | +22% | 0.003 |
| | **A4** | 7.4 ± 1.7 | 6.7 ± 1.0 | +11% | 0.13 |
| | **A5** | 12 ± 2.2 | 10.7 ± 1.3 | +12% | 0.049 |